Thermodynamic and economic analysis of the integration of high-temperature heat pumps in trigeneration systems

Luca Urbanucci[1*], Joan Carles Bruno[2], Daniele Testi[1]

[1]DESTEC (Department of Energy, Systems, Territory and Constructions Engineering), University of Pisa, Largo L. Lazzarino, 56122 Pisa, Italy

[2]Department of Mechanical Engineering, University Rovira i Virgili, Avda. Països Catalans 26, Tarragona 43007, Spain

[*]Corresponding author: luca.urbanucci@ing.unipi.it

Abstract

Polygeneration energy systems are proven to be a reliable, competitive and efficient solution for energy production. The recovery of otherwise wasted energy is the primary reason for the high efficiency of polygeneration systems. In this paper, the integration of a high-temperature heat pump within a trigeneration system is investigated. The heat pump uses the low-temperature heat from the condenser of the absorption chiller as heat source to produce hot water. A numerical model of the heat pump cycle is developed to evaluate the technical viability of current heat pump technology for this application and assess the performance of different working fluids. An exergy analysis is performed to show the advantages of the novel trigeneration system with respect to traditional systems for energy production. Moreover, a levelized cost of electricity method is applied to the proposed energy system to show its generic economic feasibility. Finally, actual energy demand data from an Italian pharmaceutical factory are considered to evaluate the economic savings obtainable with the integrated system, implemented in a case study. A two-level algorithm is proposed for the economic optimization of the investment. The synthesis/design problem is addressed by a genetic algorithm and the optimal operation problem is solved by a linear programming method. Results show that the integration of a high-temperature heat pump within a trigeneration system provides flexibility to cover variable energy demands and achieve valuable economic and energy performances, with global cost savings of around 40 % with respect to separate production and around 10 % with respect to traditional cogeneration and trigeneration systems.

Keywords:
high-temperature heat pump; CCHP; levelized cost of electricity; exergy; optimization; genetic algorithm.

1. Introduction

Polygeneration energy systems are broadly recognized as an energy efficient, environmental-friendly and cost-effective alternative to separate production. Indeed, the link between fossil fuel consumption and production of greenhouse gases imposes to pursue energy efficiency enhancement, in order to achieve both economic and environmental progresses [1].

Nevertheless, the inherent complexity of Combined Cooling Heating and Power (CCHP) systems means that selecting an appropriate system configuration (synthesis) and a proper size of the energy units (design) is critical to achieve beneficial economic, energy and environmental performances [2]. In addition to the synthesis and design issues, the operation aspect must be considered as well, since intelligent control is crucial to attain high efficiency [3]. The three levels are highly interdependent, therefore the overall analysis of a CCHP system usually results in a complex optimization problem [4].

Over the years, several works have investigated the optimization problem of polygeneration energy systems. Two main approaches to solve the problem can be distinguished: exact methods, such as Mixed-Integer Linear Programming (MILP), which are very effective and reliable but require specific formulations of the problem and can be computationally demanding for real size applications [5], and metaheuristic methods, such as Genetic Algorithm (GA) or Particle Swarm Optimization (PSO), which allow a more flexible formulation but can guarantee only near-optimal solutions [6]. Selected examples of both approaches are presented below.

A MILP-based tool for the optimization of polygeneration plants serving a cluster of buildings was developed by Piacentino and Barbaro [7]. Ameri and Besharati [8] presented a MILP model for determining the optimal size and operation of multiple CCHP systems connected to a District Heating and Cooling (DHC) network. Bischi et al. [9] proposed a MILP formulation for the optimal operation of trigeneration systems, considering detailed models for off-design behavior of the units by means of piece-wise linearization. A MILP model to optimize the layout and the operation strategies of multi energy systems integrated with storages and renewables was presented by Ma et al. [10].

Yousefy et al. [11] adopted GA to optimize the integration of a hybrid CCHP system into a commercial building. A PSO algorithm was applied by Soheyli et al. [12] to find the optimal number of the components of a hybrid trigeneration system and by Sigarchian et al. [13] to optimize the operation of a complex polygeneration system. Integrated optimization of capacity and operation of a CCHP system by means of GA was performed by Wang et al. [14]. Li et al. [15] employed a GA for the operation optimization of a trigeneration system with condensation heat recovery.

In any case, the synthesis optimization problem usually starts with a superconfiguration, which comprises all the possible types of components as well as their functional interconnections [4]. This initial layout is then reduced to the optimal configuration. Moreover, polygeneration systems can take many different configurations [16] and can include a large number of different technologies [17]. The choice of the initial superconfiguration to consider is a complex issue and deeply depends on the available energy sources, required products and energy services.

Dozens of papers have focused on the integration of different energy technologies in traditional polygeneration systems, of which a non-exhaustive set of examples is given as follows. Yang and Zhai [18] investigated the hybridization of CCHP systems with PV panels and solar thermal collectors. Maleki and Rosen [19] developed a model and an optimization procedure for hybrid wind-hydrogen CHP systems. The integration of a trigeneration system with an Organic Rankine Cycle (ORC) and a Ground Source Heat Pump (GSHP) was studied by Kang et al. [20]. A thermo-economic analysis of a solar polygeneration plant for the combined production of electricity, water, cooling and heating was developed by Leiva-Illanes et al. [21]. Ommen et al. [22] investigated possible configurations for the integration of heat pumps in district heating networks supplied by cogeneration plants.

Basic trigeneration systems are traditionally composed of a prime mover (e.g., an internal combustion engine), which provides the electric power, a heat recovery system, and a thermally-driven cooling technology [23]. The most established technology for cooling generation from recovered heat is the absorption chiller, which can be single or double effect, depending on the heating source temperature [24]. Due to the low efficiency of current absorption technologies, a high amount of heat from the condenser/absorber of the chillers must be rejected into the atmosphere, by means of cooling towers or air coolers [25].

Furthermore, High-Temperature Heat Pumps (HTHPs) is a rising technology with a large potential for waste heat utilization and reduction of CO_2 emissions [26]. At present, high-temperature heating is generally supplied by inefficient auxiliary systems, such as boilers and electric heaters. Heat pumps can replace these conventional systems and several studies [24,25,26] investigated both heat pump configurations and working fluids suitability for different sink and source temperatures. Moreover, the possibility of integrating HTHPs with reciprocating gas engines was also evaluated [30].

The main purpose and novelty of this study is to investigate the integration of high-temperature vapor-compression heat pumps in CCHP systems. The underlying concept is to recover the low-temperature heat available from the condenser/absorber of the absorption chiller and use a HTHP to pump this heat to a temperature high enough for heating applications, at expense of a reduced net power production of the whole trigeneration system. In short, a novel CCHP system is considered for the joint production of electricity, cooling and hot water. This system consists of an internal combustion engine (which produces both electricity and heating), a single-effect absorption chiller and a HTHP.

The present study aims to address four main points:

- evaluating the technical viability of current heat pump technology for this application, using natural and low Global Warming Potential (GWP) working fluids. A numerical model of the heat pump cycle is developed, and different working fluids are compared on the basis of several parameters. The implementation of an internal heat exchanger is also tested;
- investigating the operating characteristics and exergy efficiency of the system. A second-law analysis is performed to compare the proposed system to traditional systems for energy production (i.e. separate production, cogeneration, and conventional trigeneration);

- performing a preliminary economic analysis of the proposed energy system. A Levelized Cost of Electricity (LCOE) formulation [31] to evaluate the economic viability of CCHP systems against conventional technologies is considered and adapted to the system under consideration;
- assessing the economic viability of the proposed trigeneration system in a specific case study. Energy demand data from a factory of a pharmaceutical company located in Tuscany (Italy) is considered. The optimal integrated sizing and operation of the proposed trigeneration system are evaluated from the economic point of view. A two-level optimization algorithm is developed: the optimal operation problem is solved by means of a linear programming technique, while a genetic algorithm is applied to the synthesis/design problem. Results achieved with the proposed system are compared to those of traditional systems for energy production.

The rest of the paper is structured as follows. Section 2 focuses on high-temperature heat pumps for hot water production. First, the numerical model of the heat pump cycle and the working fluids are described; then, simulation results are presented, and, finally, a market overview follows. Section 3 analyzes the proposed trigeneration system with integrated high-temperature heat pump. After an energy system overview is given, the exergy analysis and the levelized cost of electricity analysis are presented. In Section 4, the case study is described; the optimization problem and methodology are illustrated in detail, and an in-depth analysis of the results is provided. The last section contains concluding remarks.

2. High-temperature heat pumps for hot water production

The definition of the temperature level of high-temperature heat pumps is not consistent in literature and market [26]. However, heat sink temperatures usually range from 85 °C to 165 °C and compression heat pumps as well as thermally driven sorption and hybrid absorption-compression heat pumps can be used.

The principle of operation of HTHPs is the exploitation of heat from low-temperature energy sources, to pump it to higher temperature levels [30]. Typical low-temperature energy sources are: waste heat from industrial processes, ground sources, flue gases, waste heat from cooling systems, and river, lake or sea water. Suitable heat sinks are: industrial processes, district heating, and domestic hot water.

Strictly related to the heat source and sink temperatures, the temperature "lift" is an important parameter to classify HTHPs. It is defined as the difference between the source and output temperatures and it has a great influence on the coefficient of performance (COP) of the device. Indeed, as well known, the COP of a Carnot heat pump cycle, which achieves the maximum theoretical performance, is highly dependent on the temperature lift.

While pure fluids keep their temperatures reasonably constant during phase changes, temperature changes can occur also at constant pressure when mixtures are employed. The temperature difference occurring in the transition from liquid to vapor (and vice versa) at constant pressure is called "glide" [32]. In this case, the theoretical limit is represented by the Lorenz cycle, which considers the temperature glide on the source and sink sides, and is equivalent to an infinite multi-stage Carnot cycle [26].

Most of the studies concerning HTHP focused on industrial working domains with sink temperatures higher than 100-120 °C. In this section, a theoretical analysis of the technical viability of vapor-compression HTHP for production of hot water (70-95 °C) is performed.

2.1 Numerical model and working fluids

In order to assess the energy performance of high-temperature heat pumps for production of hot water with different working fluids, the steady-state operation of a vapor-compression heat pump was simulated by means of a numerical cycle-based model written in MATLAB (ver. 2016b) and using the thermodynamic properties of the CoolProp database [33], which has been successfully used in the past to obtain refrigerant properties.

The numerical model is extensively based on the steady-state modeling approach by [34] and the following assumptions are considered:

- steady-state flow processes are considered;
- pure refrigerant is employed;
- pressure drops and thermal losses in pipeline are neglected;
- refrigerant pressure losses in the heat exchangers are neglected;

- the condensing and evaporating loads usually occupy at least 85 % of the heat exchange area, hence, de-superheating, sub-cooling and superheating effects are neglected in heat transfer calculations;
- water is considered as the heated fluid and the source fluid. No pressure drops in the external circuits are considered;
- evaporator and condenser approach temperatures of 5 K are considered;
- the compressor is modelled by a fixed 80 % isentropic efficiency and a fixed 80 % volumetric efficiency.

The input data of the model are as follows: working fluid, heat source fluid inlet/outlet temperatures, heat sink fluid inlet/outlet temperatures, heating capacity. Consequently, the following output data are available from the simulations: heat source fluid and heat sink fluid mass flow rates, thermodynamic states and properties of the refrigerant at the points of the cycle and refrigerant mass flow rate, heat exchangers characteristics (capacity, effectiveness and product of overall heat transfer coefficient and heat transfer area), compressor power consumption, and COP of the reverse cycle.

The inlet/outlet temperatures of the source fluid are equal to 36.5 °C and 31 °C, respectively, on the basis of the cooling water data of a typical hot-water-fired absorption chiller [35]. Indeed, as it will be explained in more detail below, the heat pump is supposed to exploit heat from the condenser/absorber of an absorption chiller.

The outlet temperature of the heated fluid is varied from 70 °C to 95 °C, to assess its effect on the reverse cycle, and the inlet temperature of the heated fluid is considered as 30 K lower than the outlet temperature.

The most important parameter to take into account in the selection of the working fluid is the COP, but also other parameters must be considered, such as: compressor suction and discharge temperatures, compressor suction and discharge pressures, pressure ratio, and volumetric heating capacity (VHC) [27]. In particular, along with the COP, the VHC represents a major economic parameter [28], since a significant part of the investment of a heat pump is related to the price of the compressor [36]. In fact, the VHC is calculated as the ratio of the heating capacity of the heat pump to the compressor displacement volume. Therefore, on one hand the COP value is strictly related to the running cost of the heat pump and on the other hand the VHC is a significant parameter in terms of the investment cost.

Moreover, the environmental impact as well as the flammability and toxicity characteristics of the working fluids must be considered for the fluid selection. Characteristics of the evaluated refrigerants, suitable for the application under investigation, are listed in Table 1.

Table 1
Properties of the evaluated working fluids [27,37]

Working fluid	Fluid type	Molecular formula	ODP	GWP 100 yr	Safety group
R717	Natural	NH_3	0	0	B2L
R718	Natural	H_2O	0	0.2	A1
R134a	HFC	$C_2H_2F_4$	0	1430	A1
R290	HC	C_3H_8	0	20	A3
R600	Natural	C_4H_{10}	0	4	A3
R600a	Natural	C_4H_{10}	0	3	A3
R601	Natural	C_5H_{12}	0	4	A3
R601a	Natural	C_5H_{12}	0	4	A3
R245fa	HFC	$C_3H_3F_5$	0	1030	B1
R1234ze(E)	HFO	$C_3F_4H_2$	0	6	A2L
R1233zd(E)	HCFO	$C_3H_2ClF_3$	0.00034	1	A1
R1234ze(Z)	HFO	$C_3F_4H_2$	0	<10	A2L

2.2 Simulation results

Fig. 1 shows how the COP varies with the outlet temperature of the hot water, for all the considered working fluids. The best theoretical performances are achieved by ammonia (R717) and water (R718), in the whole range of temperatures. Actually, water is not particularly suitable as refrigerant, since it would require a vacuum pump to extract the non-condensable gases from the condenser [38], and the pressure ratio can be too high for a single stage compressor. Nevertheless, these problems could be overcome and water has been used as refrigerant in centrifugal chillers [39], but the high compressor discharge temperature makes it unsuitable for the application under investigation.

Tables 2 and 3 show the features of the heat pump cycle for all the considered fluids, when the outlet temperature of the heated fluid is equal to 90 °C and the heating capacity is fixed at 1000 kW. The evaporator effectiveness is equal to 52.4 % in all cases.

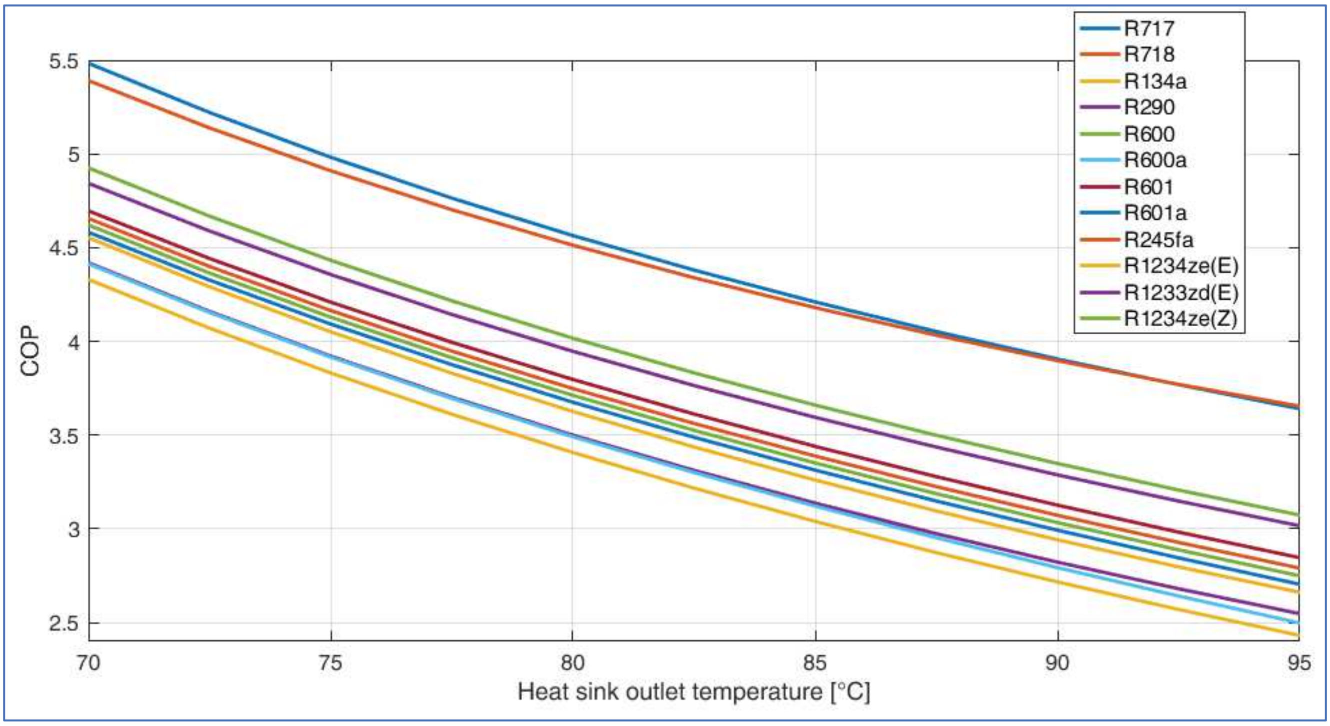

Fig. 1. Coefficient of performance vs. heat sink outlet temperature for different working fluids

Table 2
Operating parameters of refrigerants for HTHP (Part 1)

Working fluid	COP	VHC	Pressure at the condenser	Pressure at the evaporator	Pressure ratio	Maximum temperature
	-	MJ/m^3	bar	bar	-	°C
R717	3.91	7.30	47.89	10.35	4.63	169.2
R718	3.90	0.06	0.66	0.03	22.00	410.2
R134a	2.94	2.96	31.42	6.85	4.59	100.4
R290	2.82	3.45	35.84	9.77	3.67	98.9
R600	3.03	1.29	14.18	2.51	5.65	96.3
R600a	2.79	1.58	18.54	3.61	5.14	96.3
R601	3.13	0.46	5.67	0.71	7.99	98.1
R601a	2.99	0.56	7.05	0.95	7.42	98.9
R245fa	3.07	0.94	11.59	1.54	7.53	96.1
R1234ze(E)	2.72	2.13	25.91	5.14	5.04	97.0
R1233zd(E)	3.29	0.87	9.37	1.35	6.94	95.2
R1234ze(Z)	3.35	1.15	11.75	1.84	6.39	99.1

Table 3
Operating parameters of refrigerants for HTHP (Part 2)

Working fluid	Volumetric flow rate at the inlet of the compressor	Refrigerant mass flow rate	Evaporator UA	Condenser UA	Condenser effectiveness
	m^3/s	kg/s	kW/K	kW/K	%
R717	0.11	0.88	100.36	10.71	27.5
R718	13.99	0.34	100.28	2.99	8.6
R134a	0.27	9.00	89.04	45.12	74.2
R290	0.23	4.91	87.11	49.20	77.2
R600	0.62	3.93	90.43	58.55	82.7
R600a	0.51	4.75	86.61	58.30	82.6
R601	1.73	3.69	91.75	51.72	78.8
R601a	1.42	4.09	89.83	49.13	77.1
R245fa	0.84	7.44	90.99	59.21	83.1
R1234ze(E)	0.38	10.20	85.25	55.47	81.1
R1233zd(E)	0.92	6.87	93.87	64.05	85.4
R1234ze(Z)	0.69	6.32	94.61	48.55	76.7

The implementation of an internal heat exchanger (IHX) between the vapor leaving the evaporator and the liquid leaving the condenser (please refer to Fig. 2 for a schematic diagram of this configuration) may improve the performance of the cycle [26], depending on the thermo-physical properties of the working fluid.

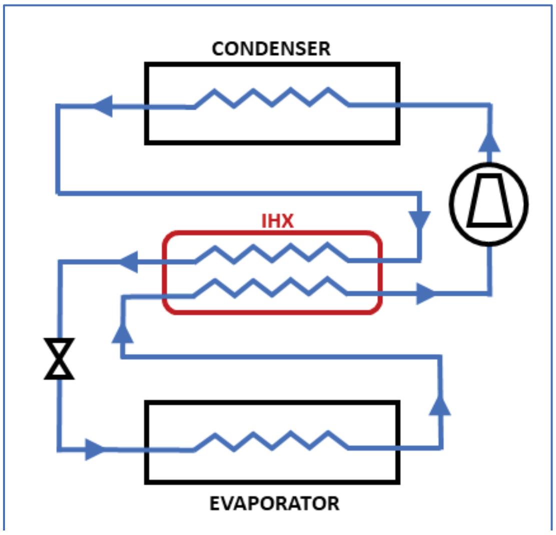

Fig. 2. Schematic of heat pump cycle with internal heat exchanger

Table 4 contains the COP values for all the tested fluids whose energy performances are improved by the IHX. The outlet temperature of the heated fluid is fixed at 90 °C and an approach temperature of 5 K is considered for the IHX. No improvement was found for ammonia and water, while performances of other fluids have significantly benefitted from the implementation of the IHX.

Table 4
Energy performances with the IHX

Working fluid	COP	Percentage increase thanks

		to the IHX
	-	%
R134a	3.40	15.6
R290	3.34	18.4
R600	3.59	18.5
R600a	3.50	25.4
R601	3.67	17.2
R601a	3.63	21.4
R245fa	3.59	16.9
R1234ze(E)	3.39	24.6
R1233zd(E)	3.66	11.2
R1234ze(Z)	3.66	9.2

On the whole, ammonia turns out to be the most suitable working fluid for the application under investigation. In fact, the high COP value, along with the excellent VHC value, suggests that ammonia heat pump systems can achieve better economical and energy performance compared to the other tested refrigerants. On the other hand, minor drawbacks are the high discharge pressure and temperature. Nevertheless, these values are still acceptable, since technological limitations for ammonia are set to 60 bar for the maximum compressor discharge pressure and to 190 °C for the maximum compressor discharge temperature [27]. Furthermore, some safety precautions should be adopted because of the toxicity of ammonia [26].

However, for higher delivered-heat temperatures (> 95°C), ammonia would not be suitable anymore, since the compressor would operate at discharge pressures above 60 bar [27].

2.3 Market overview and final considerations

The numerical results are corroborated by information about HTHP for hot water production available from market and literature overviews. In fact, ammonia is widely used in industrial heat pumps, up to about 90 °C heat sink temperature [26]. Johnson Controls manufactures ammonia-based HTHPs, using either screw [40] or reciprocating [41,42] compressors and exploiting low-temperature heat sources to produce hot water. Also Neatpump [43] (HTHP from Refrigeration star) and Plus+HEAT [44] (from Mayekawa) employ ammonia for production of hot water at around 85-90°C, with a screw and a reciprocating compressor, respectively.

In all these cases, the performances of the HTHPs are similar to one another and are in full agreement with the numerical simulations: COP values around 4.0 are declared for production of hot water at 90 °C, with 35-40 °C heat source. Heating capacities typically range from hundreds of kW to a few MW.

Therefore, ammonia will be considered as the refrigerant of the high-temperature heat pump of the proposed system. As a result of the simulations, a COP of 3.9 will be considered for heating water from 60 to 90 °C, with inlet/outlet temperatures of the source fluid equal to 36.5 °C and 31 °C, respectively. No IHX will be considered, since no improvement was found for the ammonia-based cycle.

Finally, the second-law efficiency of the heat pump cycle can be evaluated as the ratio between the assessed COP and the COP of the Lorenz heat pump cycle with the same heat source and sink temperatures [45]:

$$\Psi_{HTHP} = \frac{COP_{HTHP}}{COP_{Lorenz}} = 46\ \% \qquad (1)$$

where the COP of the Lorenz heat pump cycle for constant specific heat fluids has been evaluated as follows

$$COP_{Lorenz} = \frac{\dfrac{t_{sink,out} - t_{sink,in}}{\ln\left(\dfrac{t_{sink,out} + 273.15\,°C}{t_{sink,in} + 273.15\,°C}\right)}}{\dfrac{t_{sink,out} - t_{sink,in}}{\ln\left(\dfrac{t_{sink,out} + 273.15\,°C}{t_{sink,in} + 273.15\,°C}\right)} - \dfrac{t_{source,in} - t_{source,out}}{\ln\left(\dfrac{t_{source,in} + 273.15\,°C}{t_{source,out} + 273.15\,°C}\right)}} \quad (2)$$

3. A novel trigeneration system with integrated high-temperature heat pump

3.1 Energy system overview

As already mentioned, the main purpose of this work is to investigate the integration of a HTHP within a traditional trigeneration system. The HTHP recovers the low-temperature heat available from the condenser/absorber of the absorption chiller to produce hot water. Fig. 3 shows in detail the schematic of the proposed system in its basic configuration. It should be noted that auxiliary units may be necessary – as will be seen below – such as: an auxiliary heat rejection unit (e.g. a cooling tower) for the absorption chiller, an auxiliary boiler, and an auxiliary electric chiller.

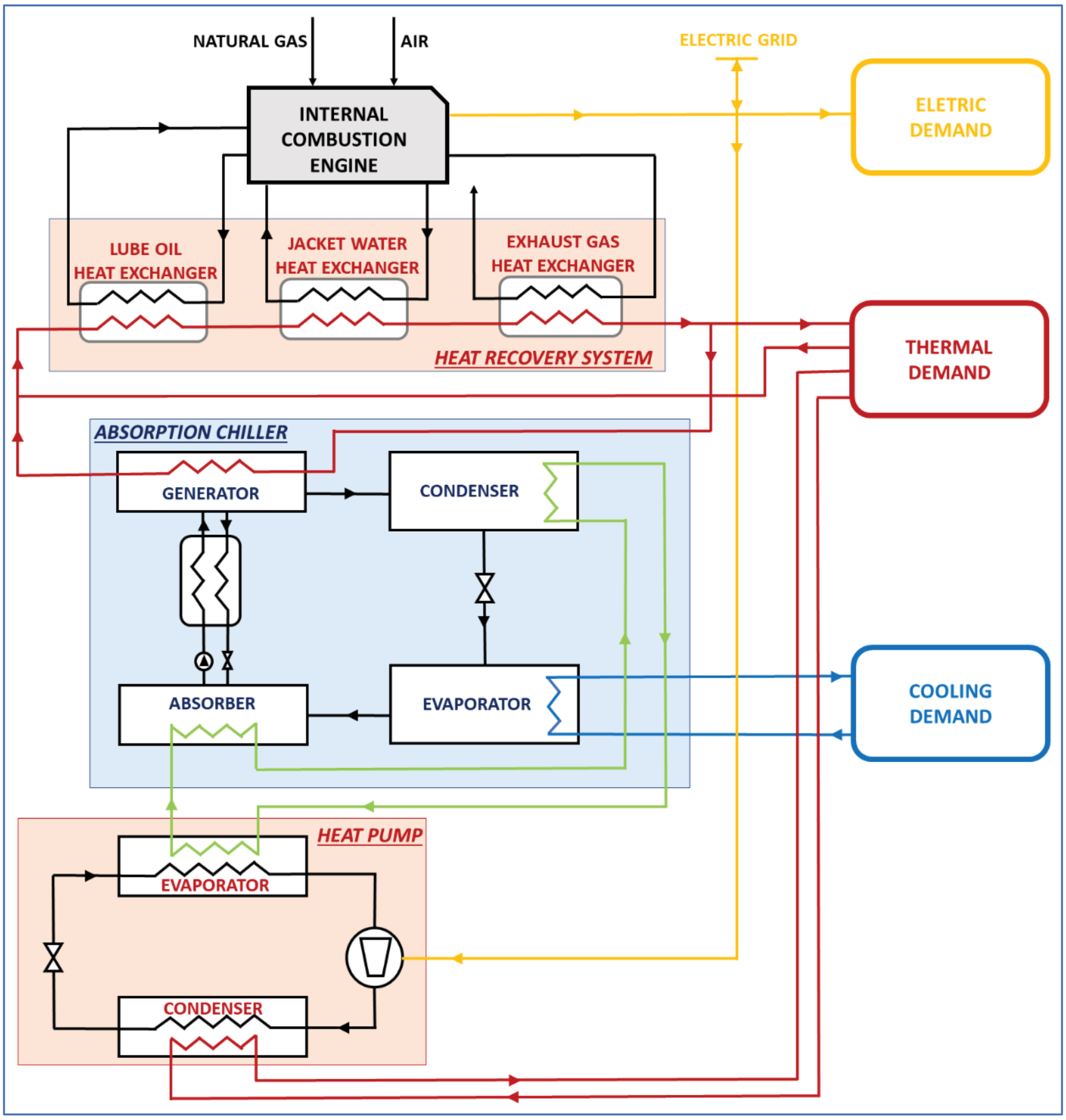

Fig. 3. Schematic of the integrated HTHP-trigeneration system: set of components

At this point, a "cascade sizing" of the system is considered. Once the nominal power of the internal combustion engine (ICE) is set, then the nominal heat recovered is known. As a consequence, the nominal cooling capacity of the absorption chiller (AC) is chosen so to use the whole recovered heat. Again, the nominal capacity of the heat pump is such to exploit the whole low-temperature heat available from the AC.

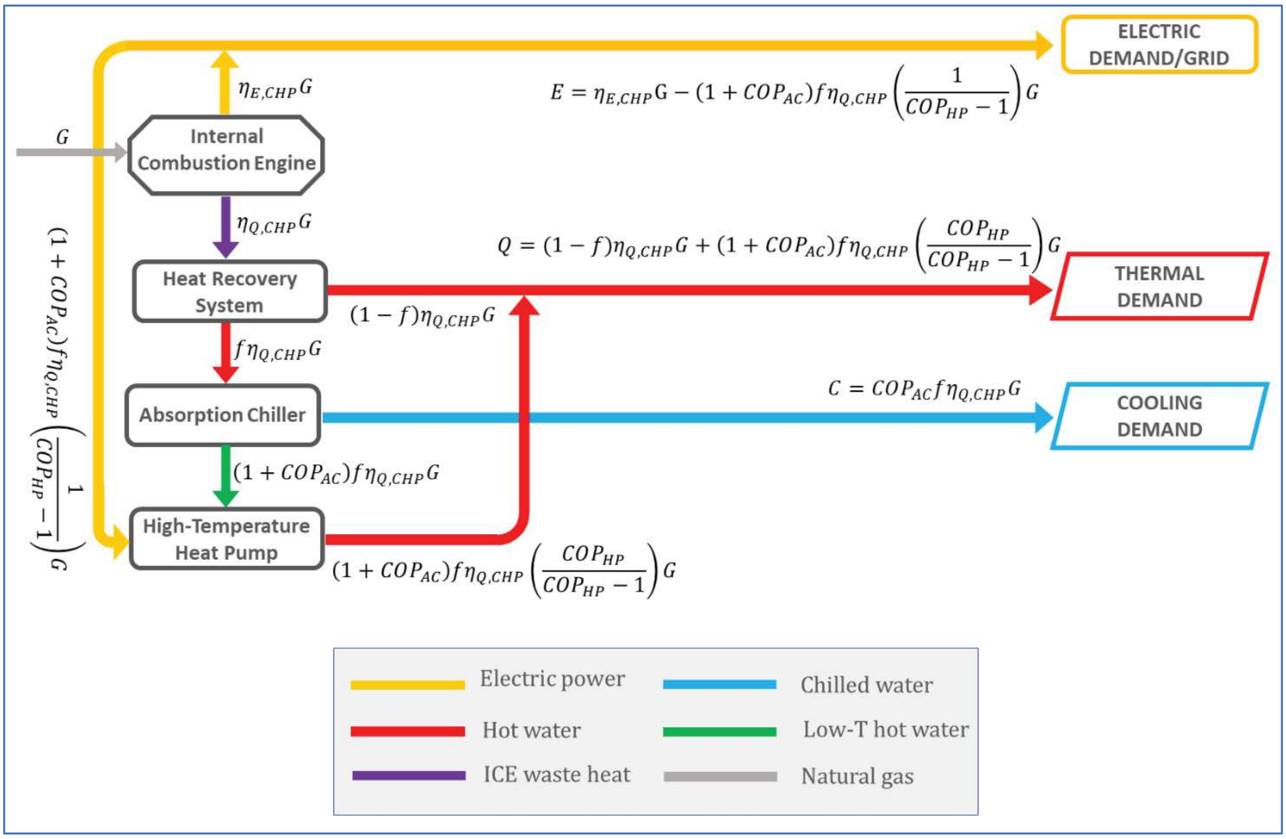

Fig. 4. Schematic of the integrated HTHP-trigeneration system: flowsheet

Fig. 4 shows another schematic representation of the proposed trigeneration system. The main energy flows are displayed and their values are reported, as a function of the fuel input G and the cogeneration recovery heat fraction to cooling f, which is the fraction of recovered heat that is used for cooling:

$$f = Q_{AC}/Q_{CHP} \tag{3}$$

This last parameter specifies how much of the heat recovered from the ICE (Q_{CHP}) feeds the absorption chiller (Q_{AC}) and, consequently, how much is directly used to satisfy the heating demand. It provides flexibility in the operation, since it is possible to modify the share of the three energy outputs to cover varying demands, by adjusting f. In this regard, Fig. 5 shows an example of how the electric, heating, and cooling production of the system may vary with f, with given values of the components efficiencies. Outputs values are normalized for the case of fuel input G equal to 1 MW.

It shall be noted that, depending on the values of efficiencies and COPs of the units, the electricity production may also be negative, above a certain value of f. This value is:

$$\tilde{f} = min\left(1, \frac{(COP_{HP}-1)\eta_{E,CHP}}{(1 + COP_{AC})\eta_{Q,CHP}}\right) \tag{4}$$

Therefore, if $f > \tilde{f}$, the energy system does not produce electric energy but, on the contrary, consumes electricity to feed the HTHP. Moreover, for the limit case in which $f = 1$, all the heat recovered from the engine is used to feed the absorption chiller (the cooling production is therefore maximized) and the heating demand is covered only by the high-temperature heat pump.

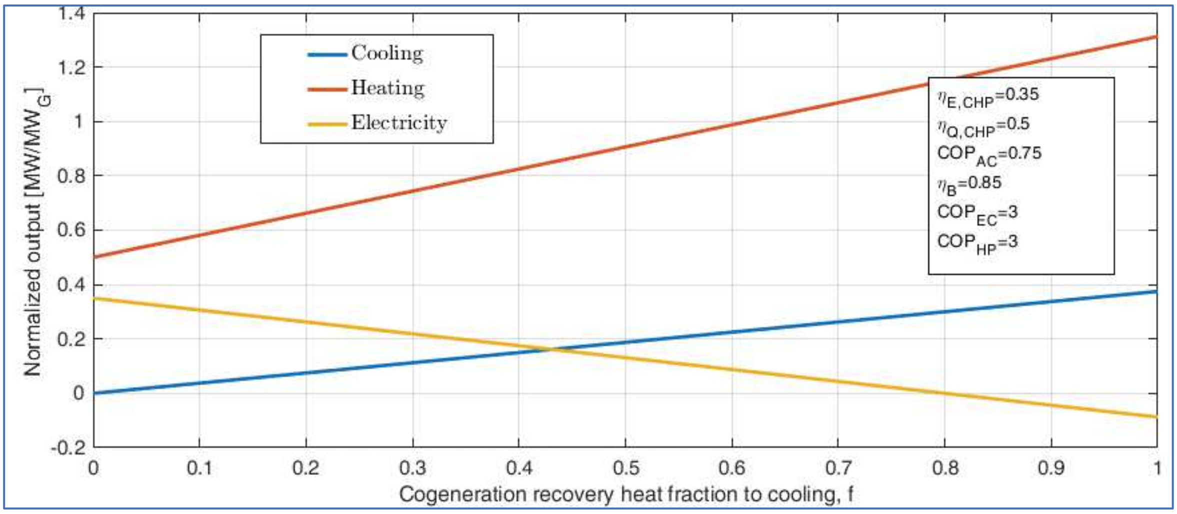

Fig. 5. Example of how the energy outputs change as the cogeneration recovery heat fraction to cooling varies, for 1 MW of input fuel (in this case, $\tilde{f} = 0.8$)

3.2 Exergy analysis

To investigate the thermodynamic performance of the proposed trigeneration system, an exergy analysis is conducted. In particular, the novel trigeneration system (schematically shown in Figs. 3-4) is compared to other traditional systems for energy production, namely separate-production system, cogeneration system, and conventional trigeneration system (which are sketched in Fig. 6).

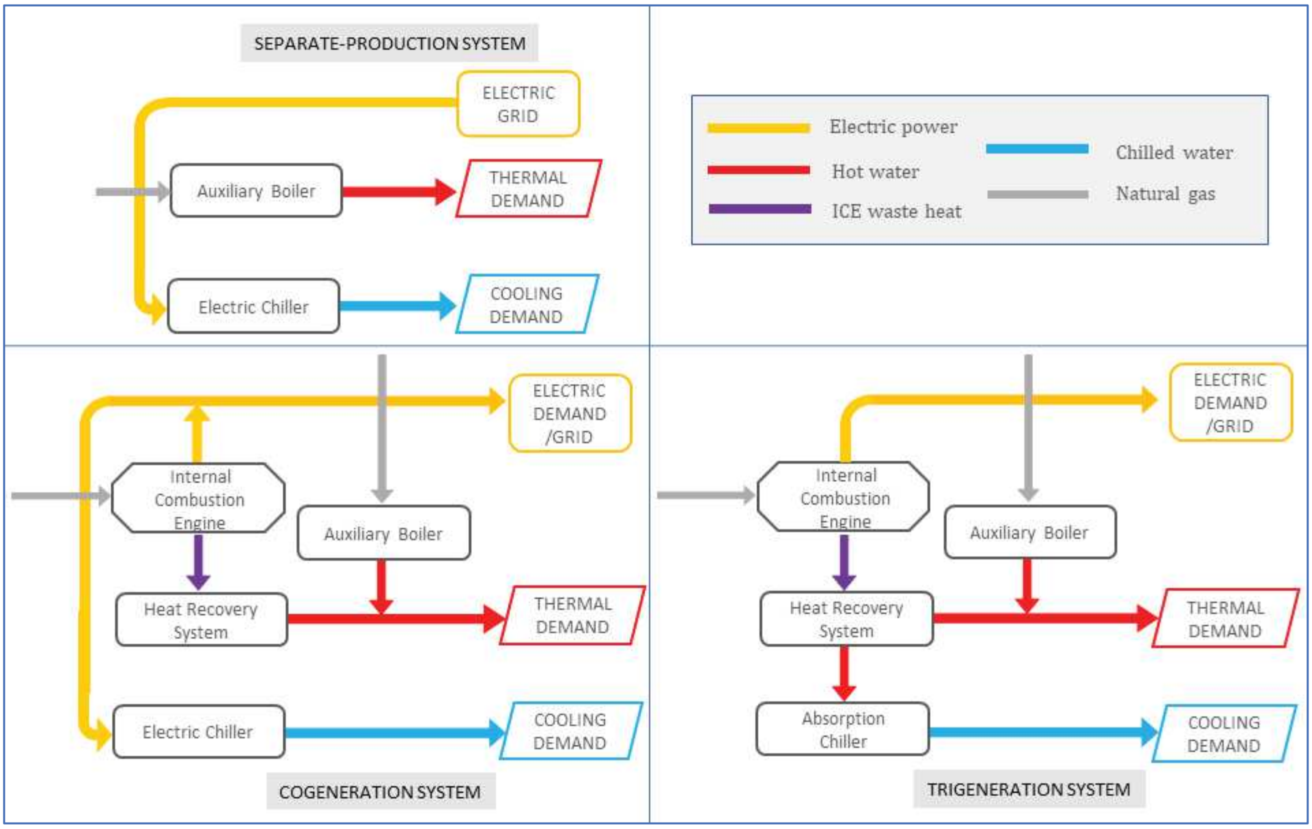

Fig. 6. Schematics of conventional systems for the production of electricity, heating, and cooling

Exergy efficiencies are calculated as the ratio between the exergy flow of the products and the exergy flow input. In order to equitably compare different system configurations, the primary exergy input to which the analysis refers is always the fuel chemical exergy. For this reason, the electric energy bought from the grid has an exergy efficiency, equal to the efficiency of a centralized thermal plant [46]:

$$\Psi_{E,ref} = \eta_{E,ref} = 38\ \%\tag{5}$$

The chemical exergy of the fuel is considered equal to its energy content, i.e. its Lower Heating Value (LHV):

$$ech_G = LHV_G\tag{6}$$

Three different outputs are considered: the electricity, whose exergy content is equal to its power, and the hot and chilled water, whose exergy contents are calculated as follows:

$$\Delta Ex_{h/c} = m_{h/c}\Delta ex_{h/c} = m_{h/c}\left[\Delta h_{h/c} - (t_0 + 273.15\ °C)\ \Delta s_{h/c}\right]\tag{7}$$

where t_0 is taken equal to 20 °C. The thermodynamic properties are calculated with CoolProp and are reported in Table 5.

The efficiencies of the components are shown in Table 6.

Table 5
Thermodynamic properties of chilled and hot water

	t_{in}	t_{out}	h_{in}	h_{out}	s_{in}	s_{out}	Δex
Chilled water	$12\ °C$	$7\ °C$	$50.6\frac{kJ}{kg}$	$29.6\frac{kJ}{kg}$	$0.181\frac{kJ}{kgK}$	$0.106\frac{kJ}{kgK}$	$0.78\frac{kJ}{kg}$
Hot water	$60\ °C$	$90\ °C$	$251.3\frac{kJ}{kg}$	$377.1\frac{kJ}{kg}$	$0.831\frac{kJ}{kgK}$	$1.193\frac{kJ}{kgK}$	$19.81\frac{kJ}{kg}$

Table 6
Units efficiencies [31]

$\eta_{E,CHP}$	$\eta_{Q,CHP}$	η_B	COP_{AC}	COP_{EC}
0.35	0.50	0.85	0.75	3.0

The exergy efficiencies of the boiler and electric chiller are, respectively:

$$\Psi_B = \frac{m_h\Delta ex_h}{m_G ech_G} = \frac{m_h\Delta ex_h}{\frac{m_h\Delta h_h}{\eta_B}} = \eta_B\left[1 - \frac{(t_0 + 273.15\ °C)\Delta s_h}{\Delta h_h}\right]\tag{8}$$

$$\Psi_{EC} = \frac{m_c\Delta ex_c}{\frac{E}{\eta_{E,ref}}} = \frac{m_c\Delta ex_c}{\frac{m_c\Delta h_c}{COP_{EC}\eta_{E,ref}}} = COP_{EC}\eta_{E,ref}\left[1 - \frac{(t_0 + 273.15\ °C)\Delta s_c}{\Delta h_c}\right]\tag{9}$$

Therefore, for the separate-production system, which comprises only the electric chiller, boiler, and electric grid, the overall exergy efficiency is

$$\Psi_{SP} = \frac{m_c\Delta ex_c + m_h\Delta ex_h + E_d}{\frac{m_c\Delta h_c}{COP_{EC}\eta_{E,ref}} + \frac{m_h\Delta h_h}{\eta_B} + \frac{E_d}{\eta_{E,ref}}}\tag{10}$$

A general definition for the exergy efficiency of conventional cogeneration and trigeneration systems and also of the proposed trigeneration system with integrated HTHP is:

$$\Psi_{CHP/CCHP/CCHP+HP} = \frac{m_c \Delta ex_c + m_h \Delta ex_h + E_d + E_s}{m_G ech_G + \frac{E_p}{\eta_{E,ref}}} \tag{11}$$

where the exergy of electricity exchanged with the grid must be considered either as an input or an output, depending on whether the system purchases electricity or sells it, respectively.

The main objective of this section is to compare, from an exergetic perspective, the proposed trigeneration system with the separate-production system, the cogeneration system, and the standard trigeneration system (all shown in Fig. 6). This comparison investigates the whole range of f varying between 0 and 1 and, therefore, the energy outputs of the proposed trigeneration system vary as f changes. If the energy outputs are normalized for the case of fuel input G equal to 1 MW, the output thermal and electric powers (in megawatts) vary as follows (refer again to Fig. 4):

$$Q = m_h \Delta h_h = (1-f)\eta_{Q,CHP} + (1+COP_{AC}) f \eta_{Q,CHP} \left(\frac{COP_{HP}}{COP_{HP}-1}\right) \tag{12}$$

$$C = m_c \Delta h_c = COP_{AC} f \eta_{Q,CHP} \tag{13}$$

$$E = \eta_{E,CHP} - (1+COP_{AC}) f \eta_{Q,CHP} \left(\frac{1}{COP_{HP}-1}\right) \tag{14}$$

As a consequence, the comparison is made considering that all the four analyzed systems produce the same Q and C and at least the same E. Besides, the cogeneration and standard trigeneration systems have the same fuel input of 1 MW to the ICE.

The proposed system comprises the HTHP, ICE, heat-recovery system, and absorption chiller; its exergy efficiency is specifically evaluated as follows:

$$\Psi_{CCHP+HP} = \frac{m_c \Delta ex_c + m_h \Delta ex_h + max\,(0, E)}{1 - \frac{min(0,E)}{\eta_{E,ref}}} \tag{15}$$

The separate-production system consists of a boiler and an electric chiller; its exergy efficiency is:

$$\Psi_{SP} = \frac{m_c \Delta ex_c + m_h \Delta ex_h + max\,(0, E)}{\frac{C}{COP_{EC}\eta_{E,ref}} + \frac{Q}{\eta_B} + \frac{max\,(0,E)}{\eta_{E,ref}}} \tag{16}$$

The cogeneration system comprises the boiler, ICE, heat-recovery system, and electric chiller; its general exergy efficiency is:

$$\Psi_{CHP} = \frac{m_c \Delta ex_c + m_h \Delta ex_h + max\left(0, E, \eta_{E,CHP} - \frac{C}{COP_{EC}}\right)}{1 + \frac{Q - \eta_{Q,CHP}}{\eta_B} - \frac{min\left(0, \eta_{E,CHP} - \frac{C}{COP_{EC}}, \eta_{E,CHP} - \frac{C}{COP_{EC}} - E\right)}{\eta_{E,ref}}} \tag{17}$$

The traditional trigeneration system, instead, comprises the boiler, ICE, heat-recovery system, and absorption chiller; its exergy efficiency is:

$$\Psi_{CCHP} = \frac{m_c \Delta ex_c + m_h \Delta ex_h + \eta_{E,CHP}}{1 + \frac{Q + \frac{C}{COP_{AC}} - \eta_{Q,CHP}}{\eta_B}} \tag{18}$$

It should be noted that with the separate-production mode it is easily possible to produce the same amount of energy outputs generated by the proposed CCHP system for all values of f; on the other hand, the cogeneration and the traditional trigeneration systems produce a surplus of electric energy compared to the proposed CCHP system for every f greater than 0. In fact, with the efficiencies of Table 6, the self-consumption of electricity by the chiller in the cogeneration system is always lower than the one by the HTHP in the proposed system. As for the standard trigeneration case, there is no self-consumption of electricity. The exergy content of this surplus of electric power is considered in their exergy efficiencies. On the contrary, no surplus of heating or cooling energy is produced by any of the systems under consideration.

Figs. 7 and 8 show how the thermal and electric power outputs and the exergy efficiencies change as f varies, for different values of the COP of the HTHP. The change of the slope of the exergy efficiencies of the separate-production and proposed trigeneration systems happens when E becomes negative. Moreover, when the COP of the HTHP is higher than 3.5, the net electric production of the system is always positive.

It should also be noted that the exergy efficiency of the proposed system is highly dependent on the value of the COP of the HTHP, and that, above a certain value of the COP (around 3.8), its exergy efficiency is always higher than the efficiency of the other systems, over the whole range of f. This is due to the fact that the proposed trigeneration system recovers the heat from the condenser/absorber of the absorption chiller, otherwise rejected. Nonetheless, if the COP of the HTHP is not sufficiently high, the recovery of heat does not compensate for the additional electricity consumption, and the exergy efficiency of the proposed system is worse than those of conventional cogeneration and trigeneration systems. Anyway, both the numerical and the market overview presented in Section 2 showed that current heat pump technology for this application achieves a COP around 4. Therefore, the proposed system can be exergetically efficient in its whole range of operation, compared to traditional systems.

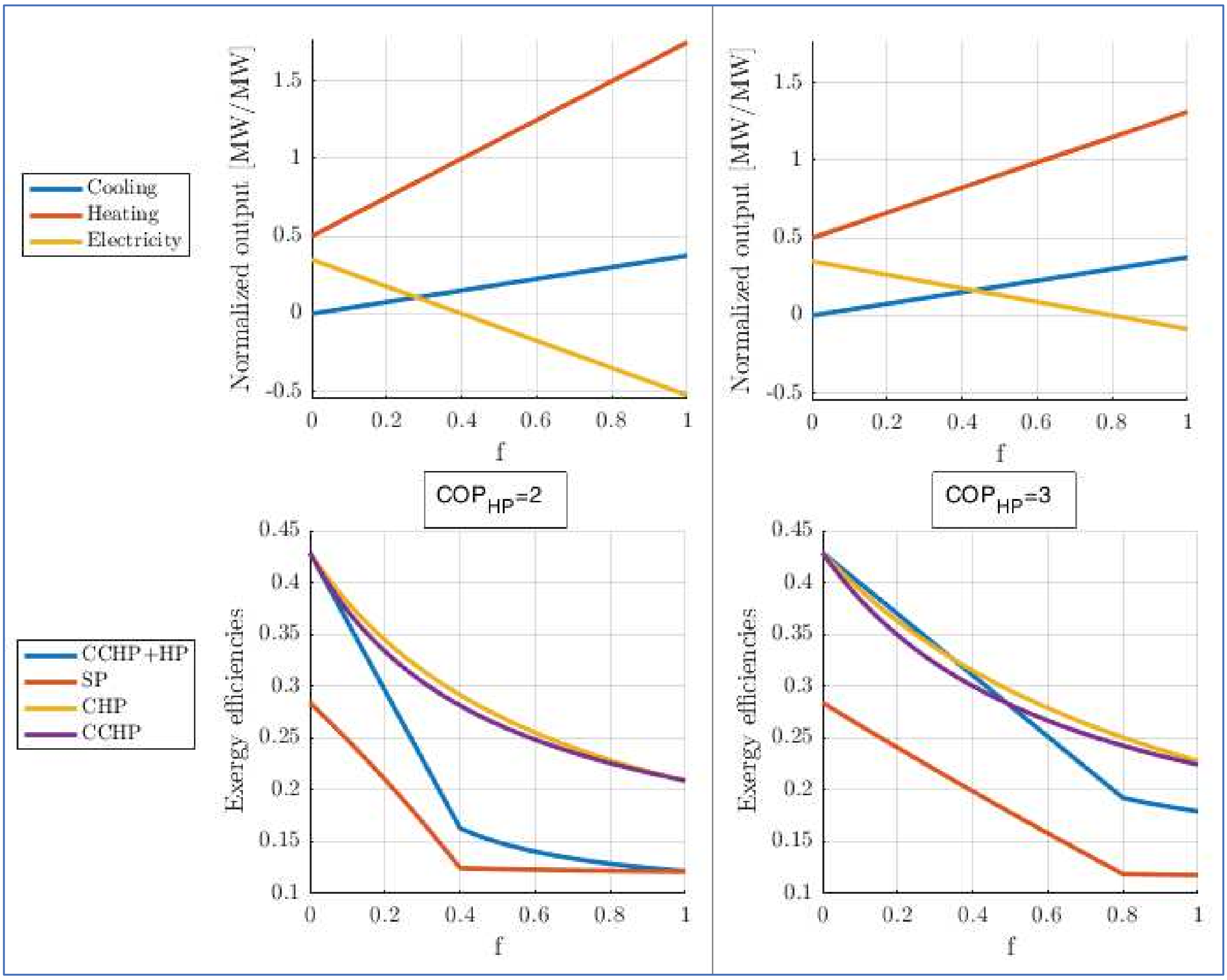

Fig. 7. Normalized energy outputs and exergy efficiencies comparison for different values of the HTHP COP (Part 1)

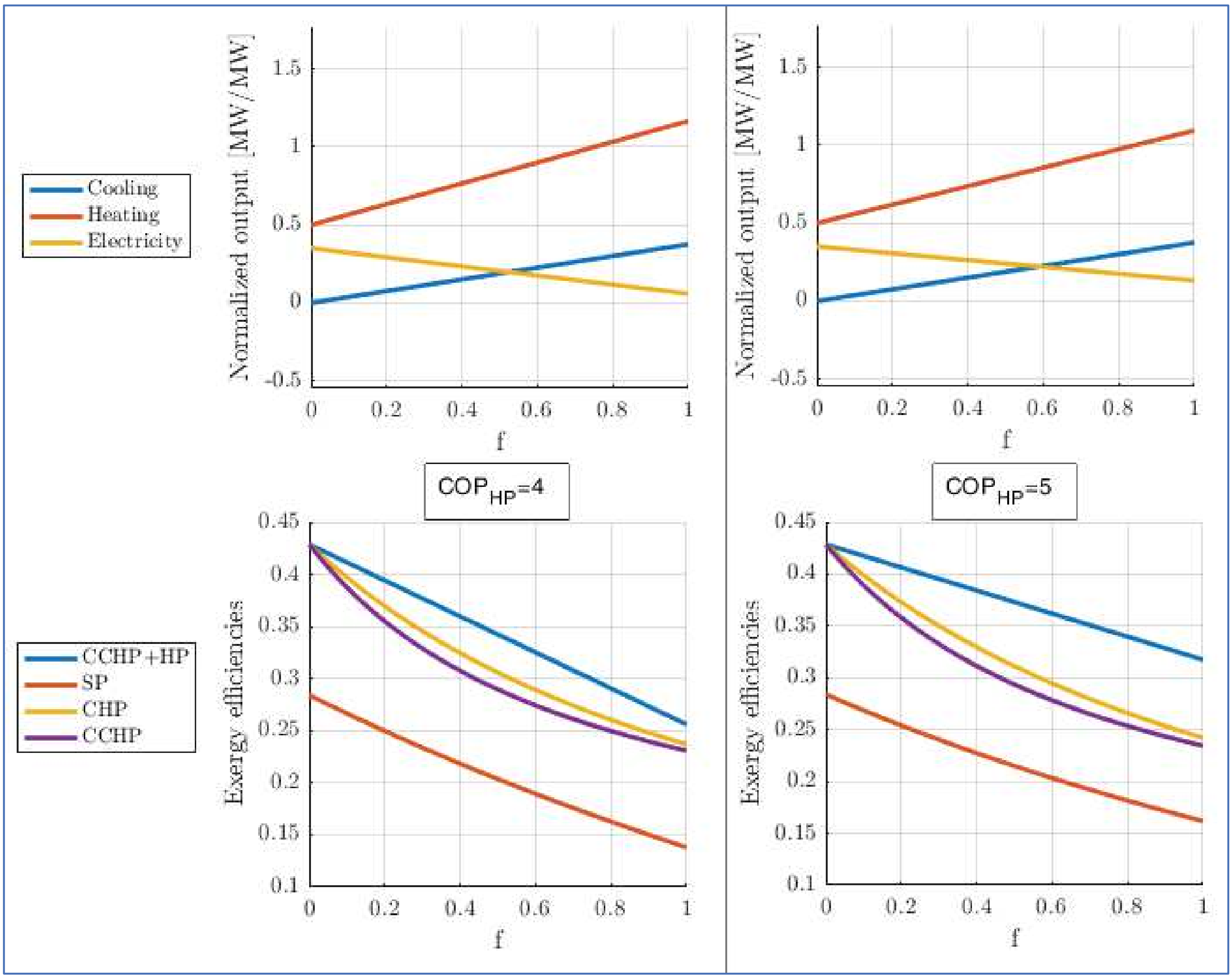

Fig. 8. Normalized energy outputs and exergy efficiencies comparison for different values of the HTHP COP (Part 2)

3.3 Levelized cost of electricity analysis

A Levelized Cost of Electricity (LCOE) method for CCHP systems [31] has been adopted to perform a preliminary economic analysis of the proposed system. This approach has been chosen because of its suitability for evaluating the generic economic viability of an energy system. In fact, net present value approaches are more appropriate for case-specific analyses.

The adopted method aims at determining the economic viability of a trigeneration system, over alternative configurations for heating and cooling. In this case, the reference system for comparison is a typical separate-production system, consisting of a boiler and an electric chiller, and the adopted method has been specifically adapted to the proposed energy system.

As explained in [31], the LCOE consists of the following five terms, all normalized per unit of produced electricity: the total investment cost of the analyzed system; the maintenance cost; the cost of fuel consumed by the ICE; the avoided cost of natural gas that the boiler would consume to generate the same amount of heating produced by the analyzed system; the avoided cost of electricity that the electric chiller would consume to produce the same amount of cooling produced by the analyzed system.

$$LCOE = \frac{CRF}{t_y \cdot CF} c_{INV} + c_{MAINT} + \frac{G}{E} c_G - \frac{G_{av,B}}{E} c_G - \frac{E_{av,E}}{E} c_E \tag{19}$$

The heating power produced by the proposed trigeneration system is:

$$Q = (1-f)\eta_{Q,CHP}G + (1+COP_{AC})f\eta_{Q,CHP}\left(\frac{COP_{HP}}{COP_{HP}-1}\right)G \tag{20}$$

With the separate-production system, the same amount of heating would be produced by the boiler:

$$Q = \eta_B G_{av,B} \tag{21}$$

Therefore, by equating those expressions, the avoided natural gas results:

$$G_{av,B} = \frac{(1-f)\eta_{Q,CHP}}{\eta_B}G + \frac{(1+COP_{AC})f\eta_{Q,CHP}}{\eta_B}\left(\frac{COP_{HP}}{COP_{HP}-1}\right)G \tag{22}$$

Analogously, the cooling production of the system is

$$C = COP_{AC}f\eta_{Q,CHP}G \tag{23}$$

With the separate-production system, the same amount of cooling would be produced by the electric chiller:

$$C = COP_{EC}E_{av,E} \tag{24}$$

Consequently, the avoided electric energy is

$$E_{av,E} = \frac{f\eta_{Q,CHP}COP_{AC}}{COP_{EC}}G \tag{25}$$

Moreover, the electricity produced by the system is

$$E = \left[\eta_{E,CHP} - (1+COP_{AC})f\eta_{Q,CHP}\left(\frac{1}{COP_{HP}-1}\right)\right]G \tag{26}$$

Therefore, it is finally possible to rearrange the LCOE expression as a function of f, as follows:

$$\begin{aligned} LCOE = {} & \frac{CRF}{t_y \cdot CF}c_{INV} + c_{MAINT} + \frac{c_G}{\eta_{E,CHP} - (1+COP_{AC})f\eta_{Q,CHP}\left(\frac{1}{COP_{HP}-1}\right)} \\ & - \left[\frac{(1-f)\eta_{Q,CHP}}{\eta_B} \right. \\ & \left. + \frac{(1+COP_{AC})f\eta_{Q,CHP}}{\eta_B}\left(\frac{COP_{HP}}{COP_{HP}-1}\right)\right]\frac{c_G}{\eta_{E,CHP} - (1+COP_{AC})f\eta_{Q,CHP}\left(\frac{1}{COP_{HP}-1}\right)} \\ & - \frac{f\eta_{Q,CHP}COP_{AC}}{COP_{EC}}\frac{c_E}{\eta_{E,CHP} - (1+COP_{AC})f\eta_{Q,CHP}\left(\frac{1}{COP_{HP}-1}\right)} \end{aligned} \tag{27}$$

Nevertheless, when all the electricity produced by the ICE is consumed by the HTHP, the LCOE expression has no meaning anymore (it diverges for $f = f_0$). Therefore, the LCOE expression must be modified in more general terms, so to be valid also for $f \geq f_0$. In order to do that, the reference electric energy produced by the system is considered equal to the electric nominal production of the ICE (see Eq. 29). Consequently, a sixth additional term must be considered in the LCOE expression, namely the cost of the electric energy feeding the high-temperature heat pump (which is shown in Eq. 30). Indeed, the polygeneration system under investigation has two energy inputs (fuel and electric energy from the grid) and three energy outputs (electricity, cooling and heating). All of them must be considered in the evaluation of the levelized cost of electricity, which becomes:

$$LCOE = \frac{CRF}{t_y \cdot CF} c_{INV} + c_{MAINT} + \frac{G}{E_{ref}} c_G - \frac{G_{av,B}}{E_{ref}} c_G - \frac{E_{av,E}}{E_{ref}} c_E + \frac{E_{HP}}{E_{ref}} c_E \tag{28}$$

$$E_{ref} = \eta_{E,CHP} G \tag{29}$$

$$E_{HP} = (1 + COP_{AC}) f \eta_{Q,CHP} \left(\frac{1}{COP_{HP} - 1} \right) G \tag{30}$$

In conclusion, the LCOE reads:

$$\begin{aligned} LCOE = {} & \frac{CRF}{t_y \cdot CF} c_{INV} + c_{MAINT} + \frac{c_G}{\eta_{E,CHP}} \\ & - \left[\frac{(1-f)\eta_{Q,CHP}}{\eta_B} + \frac{(1 + COP_{AC}) f \eta_{Q,CHP}}{\eta_B} \frac{COP_{HP}}{COP_{HP} - 1} \right] \frac{c_G}{\eta_{E,CHP}} \\ & - \frac{f \eta_{Q,CHP} COP_{AC}}{COP_{EC}} \frac{c_E}{\eta_{E,CHP}} + \frac{(1 + COP_{AC}) f \eta_{Q,CHP}}{\eta_{E,CHP}} \left(\frac{1}{COP_{HP} - 1} \right) c_E \end{aligned} \tag{31}$$

This expression is linear with f. Hence, the sign of its derivative (shown in Eq. 32) indicates the boundary value of f at which the LCOE is minimum: clearly, with a positive slope the minimum is obtained at $f = 0$, while with a negative slope the minimum is at $f = 1$.

$$\frac{d}{df}(LCOE) = \frac{\eta_{Q,CHP}}{\eta_{E,CHP}} \left(\frac{c_G}{\eta_B} - \frac{1 + COP_{AC}}{\eta_B} \frac{COP_{HP}}{COP_{HP} - 1} c_G - \frac{COP_{AC}}{COP_{EC}} c_E + \frac{1 + COP_{AC}}{COP_{HP} - 1} c_E \right) \tag{32}$$

It shall be noted that the values of $\eta_{Q,CHP}$ and $\eta_{E,CHP}$ are irrelevant for determining the sign of the derivative.

The ratio between the cost of fuel and the cost of electricity can be defined as follows:

$$R = \frac{c_G}{c_E} \tag{33}$$

Therefore, an operating mode criterion based on market conditions (energy prices) can be defined: if

$$R > \frac{\dfrac{1 + COP_{AC}}{COP_{HP} - 1} - \dfrac{COP_{AC}}{COP_{EC}}}{\dfrac{(1 + COP_{AC}) COP_{HP}}{COP_{HP} - 1} - 1} \eta_B \tag{34}$$

f should be 1 to minimize the LCOE; otherwise, f should be 0.

According to the approach by [31], the screening condition for the economic viability of a CCHP system against conventional systems is:

$$c_E \geq LCOE \tag{35}$$

which means that the cost of the electricity from the grid must be higher than the levelized cost of electricity of the polygeneration system. For the system under investigation it turns out to be:

$$c_E \geq \frac{\dfrac{CRF}{t_y \cdot CF} c_{INV} + c_{MAINT} + \dfrac{c_G}{\eta_{E,CHP}} - \left[1 - f + (1 + COP_{AC}) f \dfrac{COP_{HP}}{COP_{HP} - 1} \right] \dfrac{\eta_{Q,CHP} c_G}{\eta_B \eta_{E,CHP}}}{1 + \left(\dfrac{COP_{AC}}{COP_{EC}} - \dfrac{1 + COP_{AC}}{COP_{HP} - 1} \right) \dfrac{f \eta_{Q,CHP}}{\eta_{E,CHP}}} \tag{36}$$

In conclusion, the break-even point for the investment and maintenance costs of the high-temperature heat pump alone, which are the only additional costs with respect to a traditional trigeneration system, can be calculated. The COP of the HTHP is considered equal to 3.9, as a result of the above considerations (please refer to Section 2) and the values of the other parameters, which are shown in Table 7, are taken from [31].

Table 7
Values of the parameters for the LCOE analysis

$\eta_{E,CHP}$	$\eta_{Q,CHP}$	COP_{AC}	COP_{HP}	$\frac{CRF}{t_y \cdot CF}$	
0.35	0.50	0.75	3.9	$2.147 \cdot 10^{-5}\ h^{-1}$	
COP_{EC}	η_B	$(c_{MAINT})_{CCHP}$	c_E	c_G	$(c_{INV})_{CCHP}$
3.0	0.85	$10\ €/MWh$	$120\ €/MWh$	$40\ €/MWh$	$1.5\ €/W$

With those values, the LCOE is minimized for $f = 1$ (the cooling production by the absorption chiller and the heating production by the heat pump are maximized) and the break-even value of the investment and maintenance costs for the HTHP turns out:

$$\left(\frac{CRF}{t_y \cdot CF} c_{INV} + c_{MAINT}\right)_{HTHP} = 61 \frac{€}{MWh} \tag{37}$$

which means a break-even HTHP investment cost of around 1800 €/kW, considering the total maintenance cost of the HTHP as a fraction of the initial investment (3 % per year, with an expected life span of 20 years, in accordance with [47]). It should be noted that results from the proposed LCOE methodology heavily depend on the values of the involved parameters, which may significantly vary from country to country. In particular, both c_E and c_G are considered the most determining parameters in the economic evaluation of trigeneration systems [31]. Nevertheless, this preliminary estimate suggests that the integration of the HTHP within the trigeneration system may be economically very profitable, since the investment cost of a HTHP ranges between 250 and 800 €/kW [26].

Fig. 9 shows how the break-even HTHP investment cost (blue line) varies as a function of the COP of the HTHP. The horizontal red line represents the investment cost of the HTHP, precautionarily considered equal to 800 €/kW. In order for the proposed trigeneration system to be economically viable against separate production, the COP of the HTHP must be higher than 2.9.

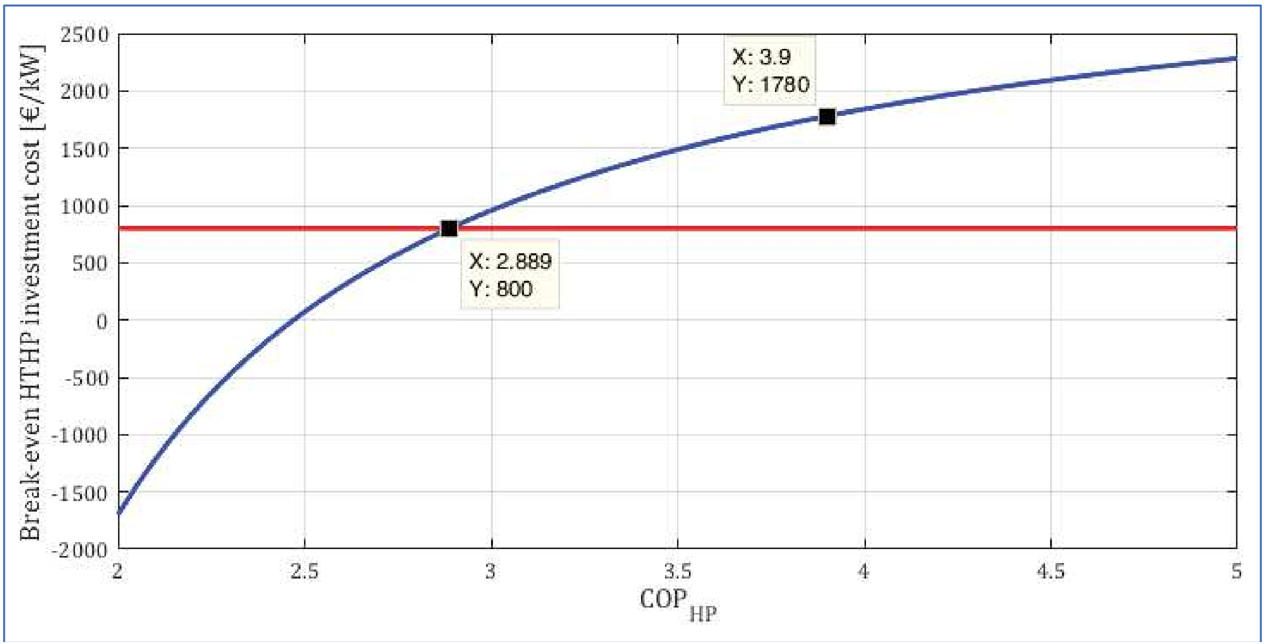

Fig. 9. Break-even HTHP investment cost as a function of the COP of the HTHP

4. Case study

4.1 Energy demand data and energy system

To analyze in more detail the economic feasibility of the proposed trigeneration system, a case study is considered. The integration of the proposed trigeneration system into an existing separate-production plant is investigated through the economic optimization of the investment.

Energy demand data from a factory of a pharmaceutical company located in Tuscany (Italy) are considered and shown in Fig. 10. In this plant, three energy services are needed for industrial activities and HVAC requirements: electricity, cooling (chilled water at 7 °C), and heating (hot water at 90 °C). Currently, these three energy services are met by electric grid, electric chillers, and boilers, respectively. The particularity of this plant is that heating and cooling are needed throughout the year, although in variable proportions. The demand for electricity is much more regular.

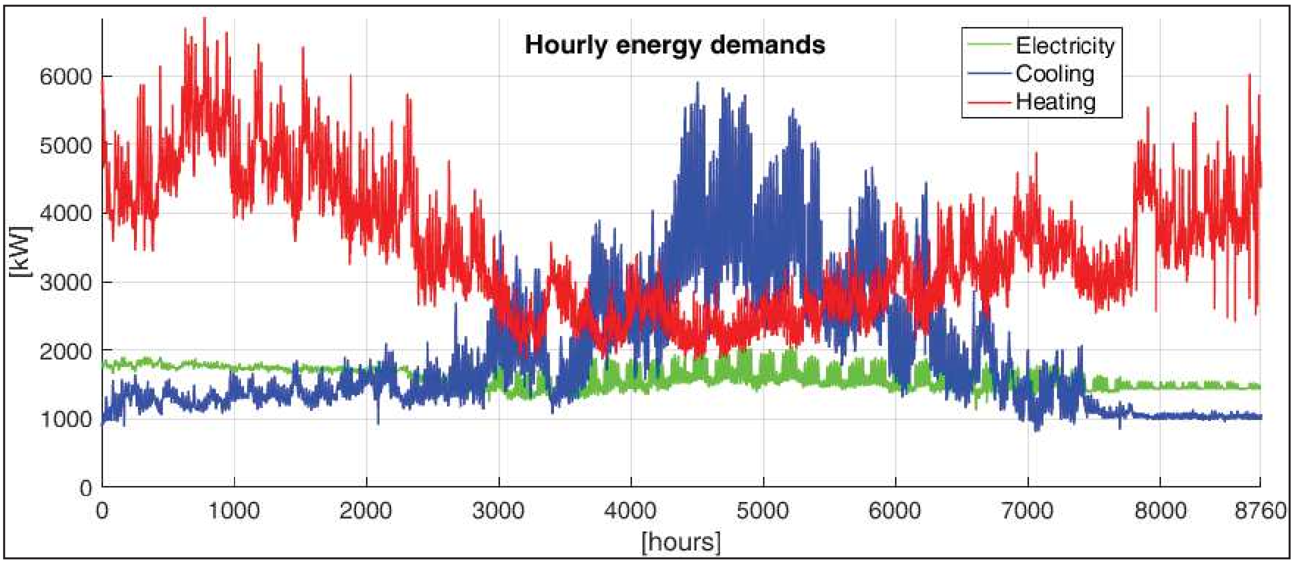

Fig. 10. Hourly energy demand data of the case study

The considered energy system superconfiguration, which is shown in Fig. 11, comprises the units and network that are already present (auxiliary boiler, electric chiller, and electric grid), and the new units to be installed (internal combustion engine, absorption chiller, and high-temperature heat pump).

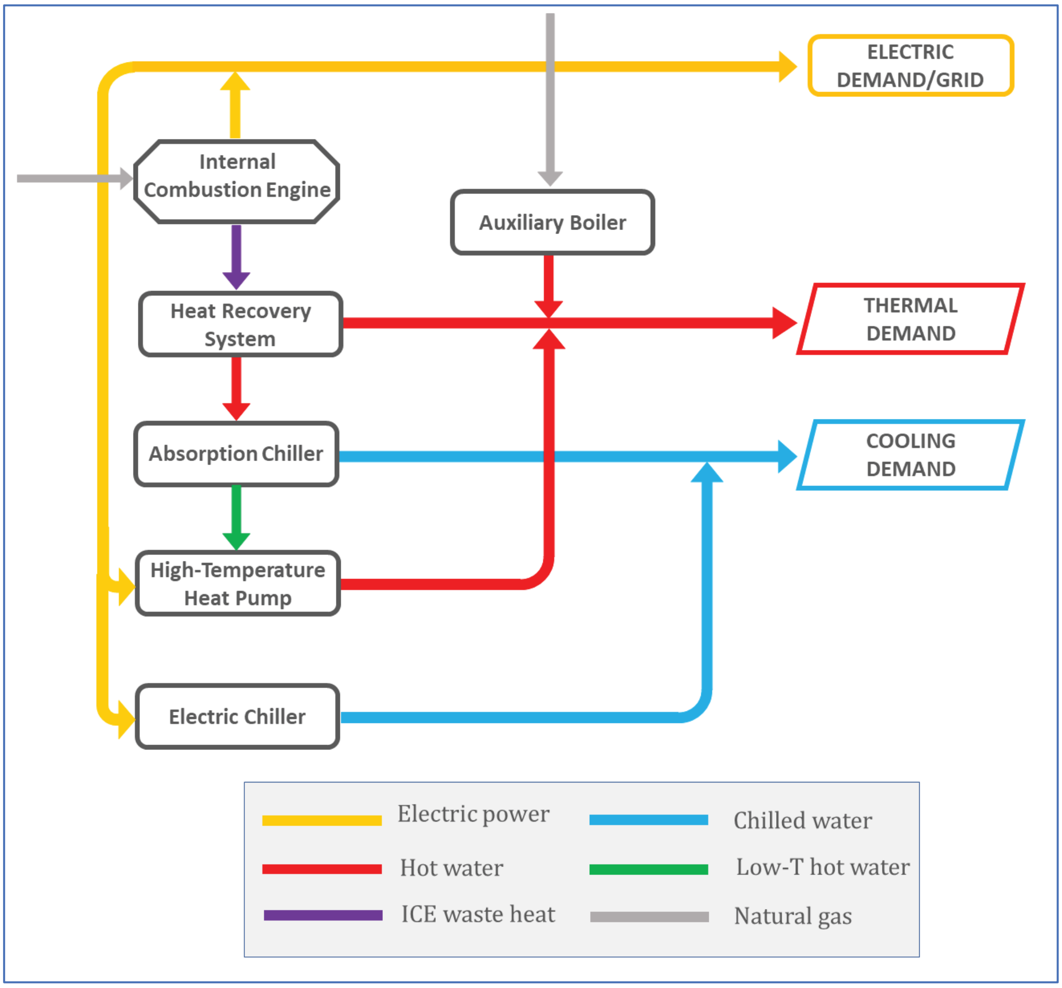

Fig. 11. Schematic of the considered superconfiguration

4.1 Optimization problem and methodology

The objective function to minimize is the Equivalent Annual Cost (EAC) of the system, which is calculated over the period of a year and composed of the annualized investment cost for the technologies, $Invest$, and the total annual operating cost, Op [48].

$$EAC: f = Invest + Op \tag{38}$$

$$Invest = \sum_{i=1}^{3} a_i CAP_i^{b_i} \cdot CRF_i \tag{39}$$

where CAP_i is the capacity of the i-th technology to be installed (expressed in kW), a_i and b_i are the correlation parameters of the equipment cost as a function of the capacity, and CRF is the capital-recovery factor [49]:

$$CRF_i = \frac{r(r+1)^{lifetime_i}}{(r+1)^{lifetime_i} - 1} \tag{40}$$

The total annual operating cost comprises the cost for purchasing electricity and natural gas and the revenue from selling electricity to the grid. An hourly timestep has been considered.

$$Op = \sum_{t=1}^{8760} [c_G(G_{CHP,t} + G_{B,t)} + c_{PE}E_{P,t} - c_{SE}E_{S,t}] \tag{41}$$

As already mentioned, the optimization variables can be distinguished in two main groups: sizing variables ($Q_{HP,nom}, E_{CHP,nom}, C_{AC,nom}$) and operating variables ($E_{CHP,t}, E_{S,t}, E_{P,t}, C_{AC,t}, C_{EC,t}, Q_{B,t}, Q_{HP,t}$, with $t = 1, \dots, 8760$).

Demand constraints must be satisfied in each t-*th* timestep:

$$Q_{HP,t} + Q_{B,t} + Q_{CHP,t} - Q_{AC,t} \geq Q_t \tag{42}$$

$$C_{AC,t} + C_{EC,t} \geq C_t \tag{43}$$

$$E_{CHP,t} + E_{P,t} - E_{S,t} - E_{EC,t} - E_{HP,t} - E_{CT,t} = E_t \tag{44}$$

where the electric consumption due to the cooling tower fans depends on the amount of heat to be rejected:

$$E_{CT} = \left[C_{AC}\left(\frac{1 + COP_{AC}}{COP_{AC}}\right) - Q_{HP}\left(\frac{COP_{HP} - 1}{COP_{HP}}\right) + C_{EC}\left(\frac{1 + COP_{EC}}{COP_{EC}}\right)\right] w_{CT} \tag{45}$$

It must be noted that Eq. (45) contains a negative term; in fact, when the HTHP works, it uses all or part of the low-temperature heat from the condenser/absorber of the absorption chiller, which, therefore, does not have to be rejected from the cooling tower.

Other constraints and equations for the model must be considered:

$$C_{AC,t}/COP_{AC} \leq Q_{CHP,t} \tag{46}$$

$$Q_{HP,t}\left(\frac{COP_{HP} - 1}{COP_{HP}}\right) \leq C_{AC,t}\left(\frac{COP_{AC} + 1}{COP_{AC}}\right) \tag{47}$$

$$C_{AC,t} \leq C_{AC,nom} \tag{48}$$

$$C_{EC,t} \leq C_{EC,nom} \tag{49}$$

$$E_{CHP,t} \leq E_{CHP,nom} \tag{50}$$

$$Q_{CHP,t} = E_{CHP,t}\frac{\eta_{Q,CHP}}{\eta_{E,CHP}} \tag{51}$$

$$G_{CHP,t} = E_{CHP,t}/\eta_{E,CHP} \tag{52}$$

$$Q_{HP,t} \leq Q_{HP,nom} \tag{53}$$

$$Q_{B,t} \leq Q_{B,nom} \tag{54}$$

$$G_{B,t} = Q_B/\eta_B \tag{55}$$

$$C_{AC,nom}/COP_{AC} \leq Q_{CHP,nom} \tag{56}$$

$$Q_{HP,nom}\left(\frac{COP_{HP} - 1}{COP_{HP}}\right) \leq C_{AC,nom}\left(\frac{COP_{AC} + 1}{COP_{AC}}\right) \tag{57}$$

The electric and thermal efficiencies of the internal combustion engine, in the range from 100 kW to 9 MW, vary with the nominal power of the ICE itself as follows (on the basis of data from [50]):

$$\eta_{E,CHP} = 39.66\, exp\left(5.179 \cdot 10^{-6}\, E_{CHP,nom}[kW]\right) - 14.67\, exp\left(-1.51 \cdot 10^{-3}\, E_{CHP,nom}[kW]\right) \tag{58}$$

$$\eta_{Q,CHP} = 39.85\, exp\left(-1.405 \cdot 10^{-5}\, E_{CHP,nom}[kW]\right) + 15.98\, exp\left(-1.797 \cdot 10^{-3}\, E_{CHP,nom}[kW]\right) \tag{59}$$

The COP of the single-effect hot-water fired absorption chiller can be considered constant and equal to 0.81 in the cooling capacity range from 250 kW to 4500 kW (on the basis of LG Catalogue [35]). The COP of the HTHP is considered equal to 3.9, on the basis of the considerations discussed in Section 2. The other values adopted for the simulations are shown in Table 8.

Table 8
Values adopted for the optimization

Parameter	a_{CHP}	b_{CHP}	a_{AC}	b_{AC}	η_B	c_G	c_{PE}
Value	5896 (extrapolated from [50]	0.86 (extrapolated from [50])	3575 (extrapolated from [51])	0.65 (extrapolated from [51])	0.8	0.04 €/kWh [52]	0.15 €/kWh [52]
Parameter	a_{HP}	b_{HP}	r	$lifetime$	COP_{EC}	c_{SE}	w_{CT}
Value	2615 (extrapolated from [22,24])	0.72 (extrapolated from [22,24])	0.02 [53]	20 years [53]	2.8	0.05 €/kWh [52]	0.026 kW/kW [24]

Finally, the overall problem consists in the minimization of the Equivalent Annual Cost:

$$minimize\,\{f = EAC\}$$

which results in a non-linear optimization problem, because of the non-linear variations of the nominal efficiencies of the ICE in relation to its size and of the components unitary costs in relation to their sizes.

To this aim, a two-level optimization algorithm has been developed. Indeed, as schematically summarized in Fig. 12, the overall optimization problem can be decomposed in a lower level, the optimum operation problem, and a higher level, the optimum synthesis/design problem. In the lower level, the optimal operating conditions of the system in each timestep are identified, while in the higher level, the synthesis/design problem determines which units should be included in the energy system and their size. Nevertheless, the two subproblems are nested in each other; therefore, they need to be solved simultaneously. The optimal operation problem is solved by means of a Linear Programming (LP) technique, while the synthesis/design problem is addressed by a Genetic Algorithm (GA). For each individual solution (triplet of ICE, AC, and HTHP sizes) produced by the GA, the optimal annual operation cost is evaluated by the LP solver, and, consequently, the total EAC is calculated. This procedure is repeated for each individual of each generation produced by the GA, until the stopping criteria is met. Indeed, the GA generates a population of candidate solutions at each iteration (or generation), which evolve towards better solutions by means of selection, mutation, and crossover operations.

Discrete sizes, as multiples of 100 kW, have been considered. Moreover, part-load behavior and minimum load operation of the units have been neglected and constant efficiencies have been considered. These assumptions clearly induce some errors, but they were made necessary by the linear formulation and computational issues.

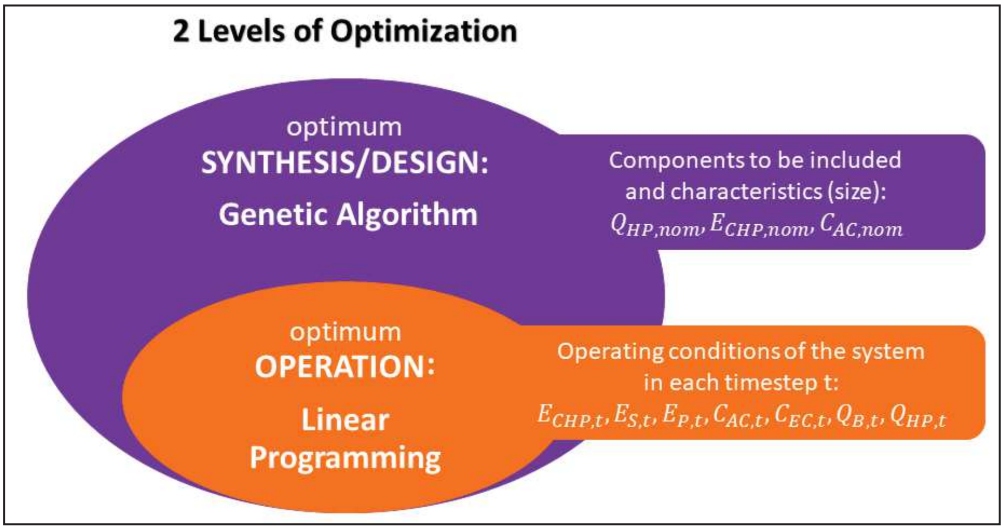

Fig. 12. Outline of the optimization algortihm

All the simulations and optimizations are performed using scripts written in MATLAB environment. The commercial solver CPLEX [54] for the linear optimization and the MATLAB Genetic Algorithm Solver [55] have been used. Settings and parameters adopted for the optimization algorithms are shown in Table 9.

Table 9
Settings and parameters adopted for the optimization algorithms

Linear Optimization	*Algorithm*			*Max iterations*		*Optimality tolerance*
	$Interior - point - legacy$			85		10^{-8}
Genetic Algorithm	*Population size*	*Elite count*	*Crossover fraction*	*Mutation function*	*Max generations*	*Max stall generations*
	150	7	0.8	$Gaussian$	300	50

4.2 Results

In addition to the superconfiguration shown in Fig. 11, also other configurations have been considered as benchmarks for comparison, namely traditional trigeneration and cogeneration systems and separate production, which have been shown in Fig. 6.

Fig. 13 compares the optimal Equivalent Annual Costs obtained with the different system configurations. The proposed trigeneration system with integrated high-temperature heat pump achieves the best performance, providing 10.3 %, 10.6 %, and 41.7 % savings in comparison to traditional CCHP, CHP, and separate-production systems, respectively. Sizing and operation of traditional trigeneration and cogeneration systems have been optimized to minimize the EAC as well.

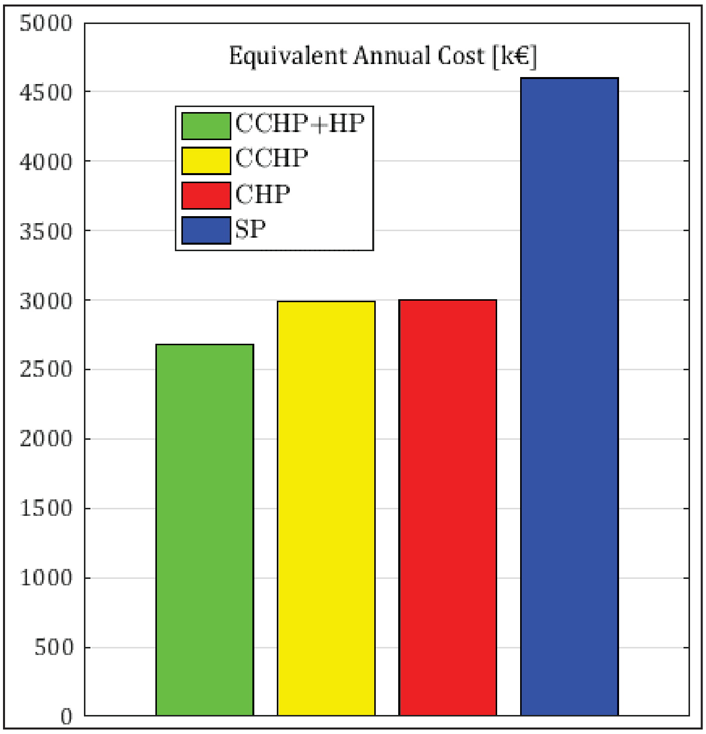

Fig. 13. Equivalent annual costs of the different systems

Table 10 summarizes the main results achieved with the optimization procedure. Optimal sizing and costs of the different configurations are shown. The size values refer to the electric, cooling, and heating capacities of the ICE, AC, and HTHP, respectively. Compared to the basic trigeneration system, the possibility of including the HTHP allows the installation of an absorption chiller of larger capacity, entailing more production of thermal energy from recovered heat and a reduced use of the boiler and electric chiller.

Moreover, even though the optimization is based on an economic objective function, the proposed trigeneration system achieves also the best energy performance: its annual primary energy consumption is 14.7 %, 14.9 %, and 39.1 % lower than CCHP, CHP, and SP consumptions, respectively. The primary energy factor for electricity has been considered equal to the electric energy efficiency shown in Eq. (5).

Table 10
Optimal Equivalent Annual Cost sizing and operation: results

	CCHP + HP	**CCHP**	**CHP**	**SP**
Internal Combustion Engine	2800 kW	2800 kW	3000 kW	/
Absorption Chiller	1900 kW	300 kW	/	/
High-Temperature Heat Pump	3900 kW	/	/	/
Boiler: peak heating production	1888 kW	4660 kW	4673 kW	6859 kW
Electric chiller: peak cooling production	4014 kW	5696 kW	5914 kW	5914 kW
Annual Operation Cost	2261 k€	2649 k€	2650 k€	4603 k€
Annualized Investment Cost	423 k€	341 k€	353 k€	0 k€
Equivalent Annual Cost	**2684 k€**	**2990 k€**	**3003 k€**	**4603 k€**
Annual Primary Energy Consumption	**56030 MWh**	**65670 MWh**	**65850 MWh**	**92020 MWh**

Figs. 14-16 show how the electric, heating, and cooling demands are met with the proposed trigeneration system, under the optimal economic sizing and operational strategy, over the whole year, on hourly timesteps. The boiler and the electric chiller work only to meet peak demands, while the high-temperature heat pump and the absorption chiller provide the base load. Moreover, the purchasing of electricity from the grid is almost exclusively intended to feed the electric chiller, therefore occurring at the same time of cooling peak demands.

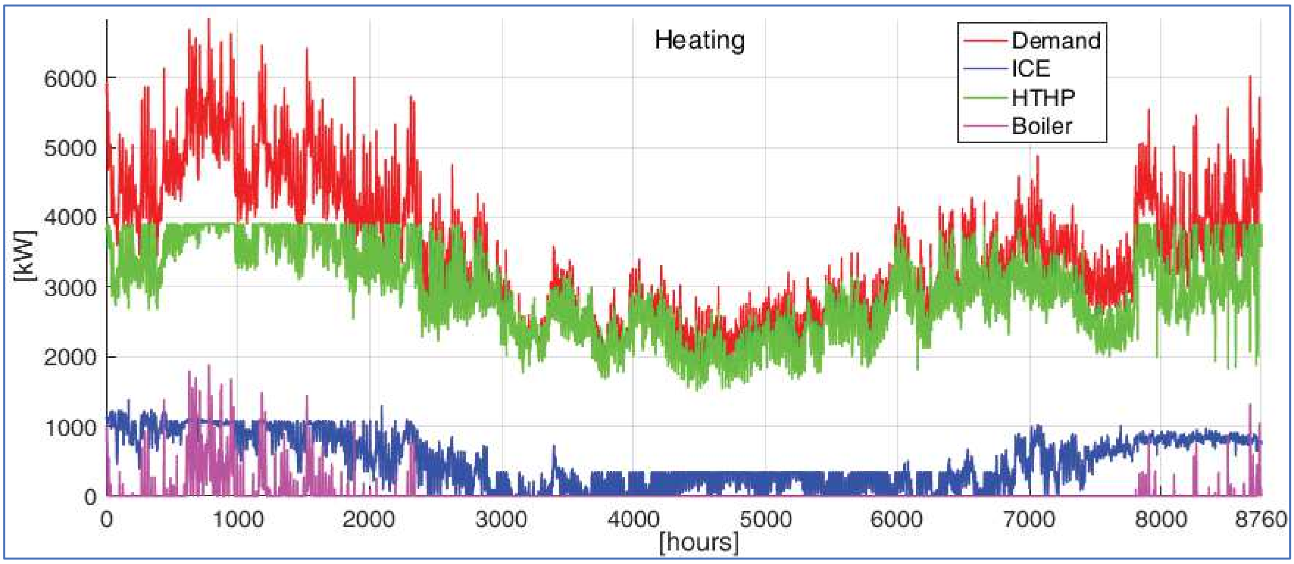

Fig. 14. Optimization results: the annual hourly heating loads with the CCHP+HP system

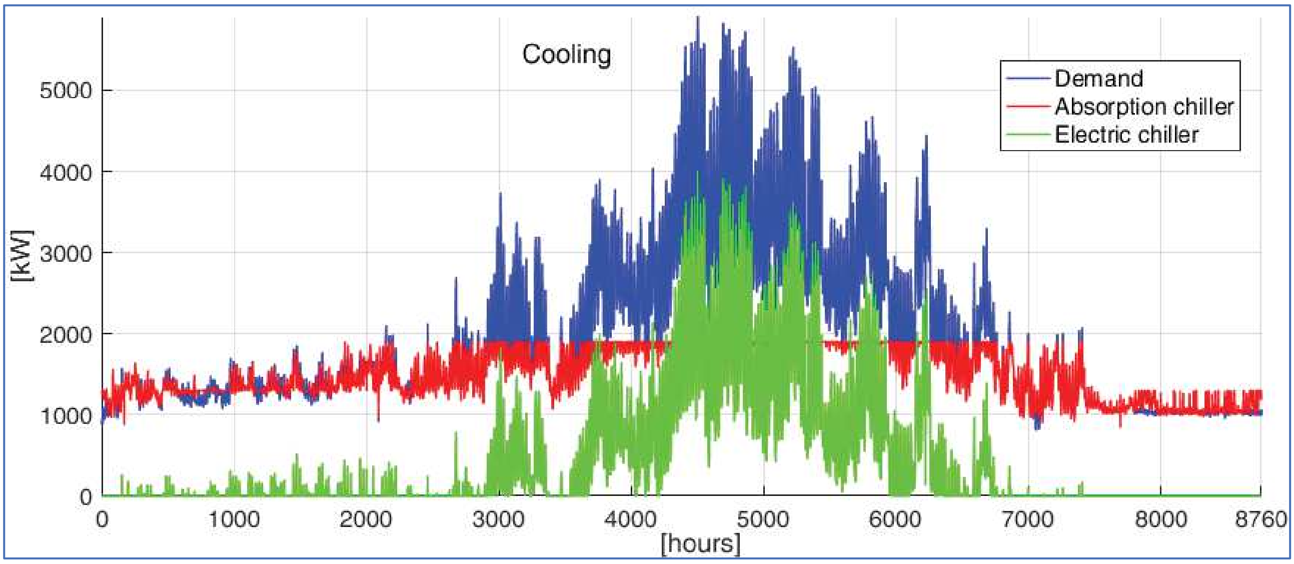

Fig. 15. Optimization results: the annual hourly cooling loads with the CCHP+HP system

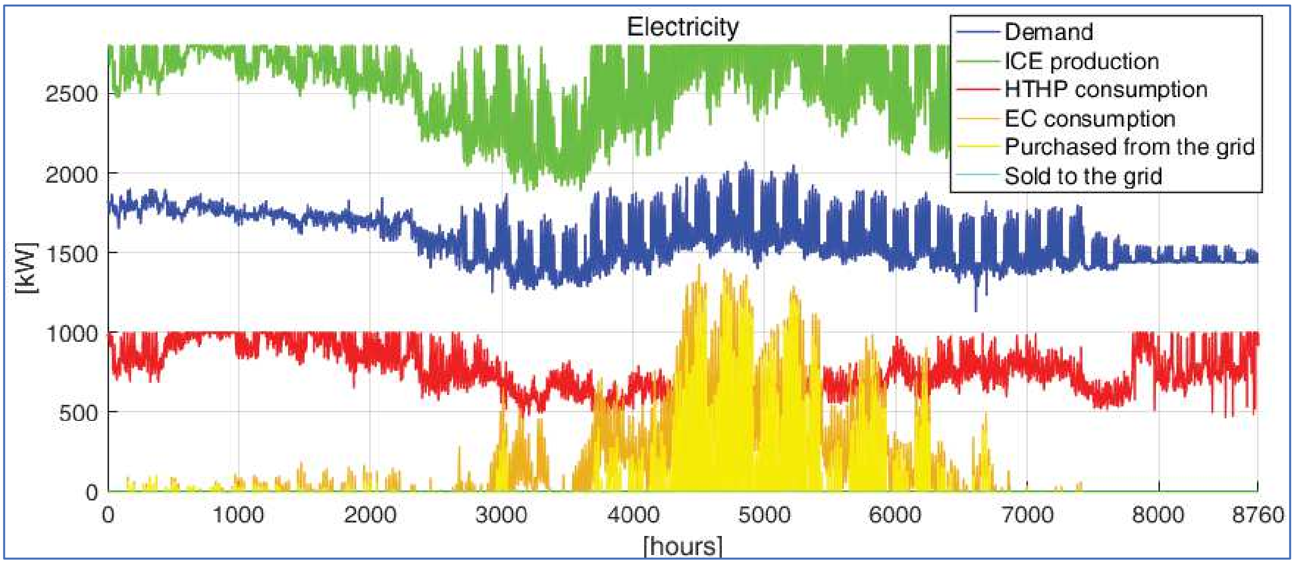

Fig. 16. Optimization results: the annual hourly electric loads with the CCHP+HP system

Furthermore, Fig. 17 compares how the optimal cogeneration recovery heat fraction to cooling, f, varies throughout the year for the integrated CCHP-HTHP system and for the basic CCHP system. This chart highlights how the high-temperature heat pump allows a much larger exploitation of the thermally-driven cooling technology. In fact, the recovery of low-temperature heat from the absorption chiller makes the energy system significantly more efficient. Without the HTHP, the heat recovered from the ICE is mostly used directly to meet the heating demand (to avoid the use of the boiler) and the cooling demand is almost entirely met by the electric chiller.

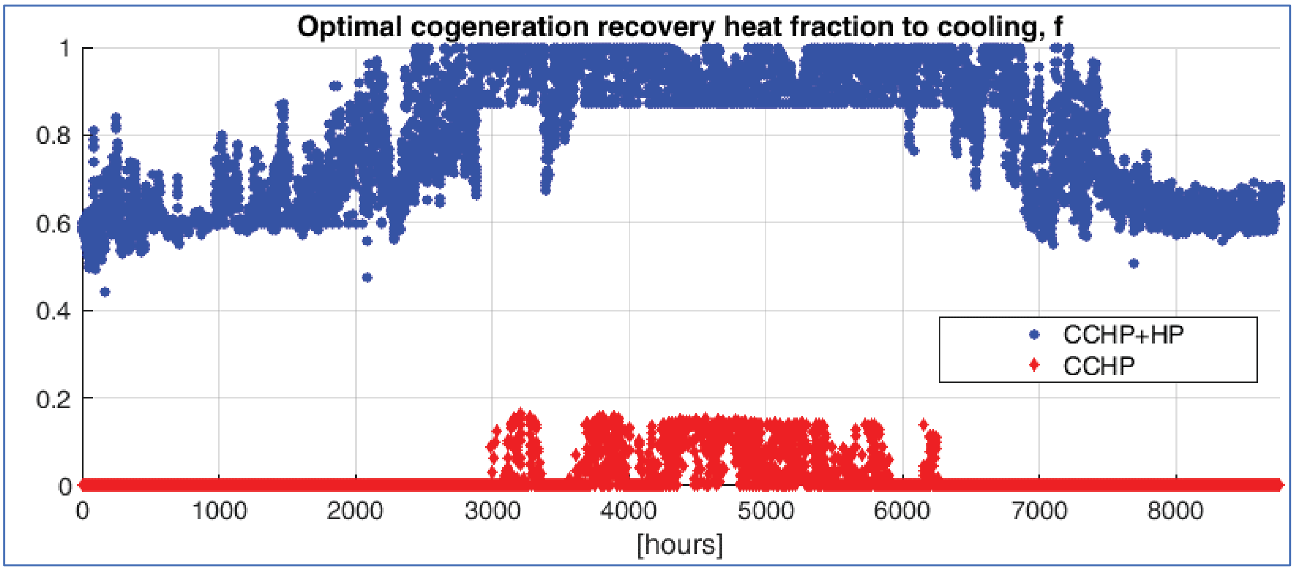

Fig. 17. Optimal cogeneration recovery heat fraction to cooling: comparison between the CCHP+HP and CCHP systems

Figs. 18-19 allow an in-depth analysis of the operational interaction between the absorption chiller and the high-temperature heat pump. In particular, Fig. 18 shows how the exhausted heat from the condenser/absorber of the absorption chiller is shared among the evaporator of the high-temperature heat pump and the cooling tower, in each hourly timestep. The heat available at the evaporator of the HTHP is either larger or slightly smaller than its nominal value; this means that the heat pump can work at its nominal conditions – or very close to them – for most of the year.

Fig. 19, instead, provides an insight into the ratio between the heat at the evaporator (i.e. heat source) of the high-temperature heat pump and the whole exhausted heat from the condenser/absorber of the absorption chiller. The annual hourly values, the duration curve, and the average value are shown. It can be seen that most of the exhausted heat is recovered as heat source for the heat pump, thus reducing the utilization of the cooling tower. Predictably, lower values of the parameter occur during the summer, when the ratio between the cooling and the thermal demand is higher.

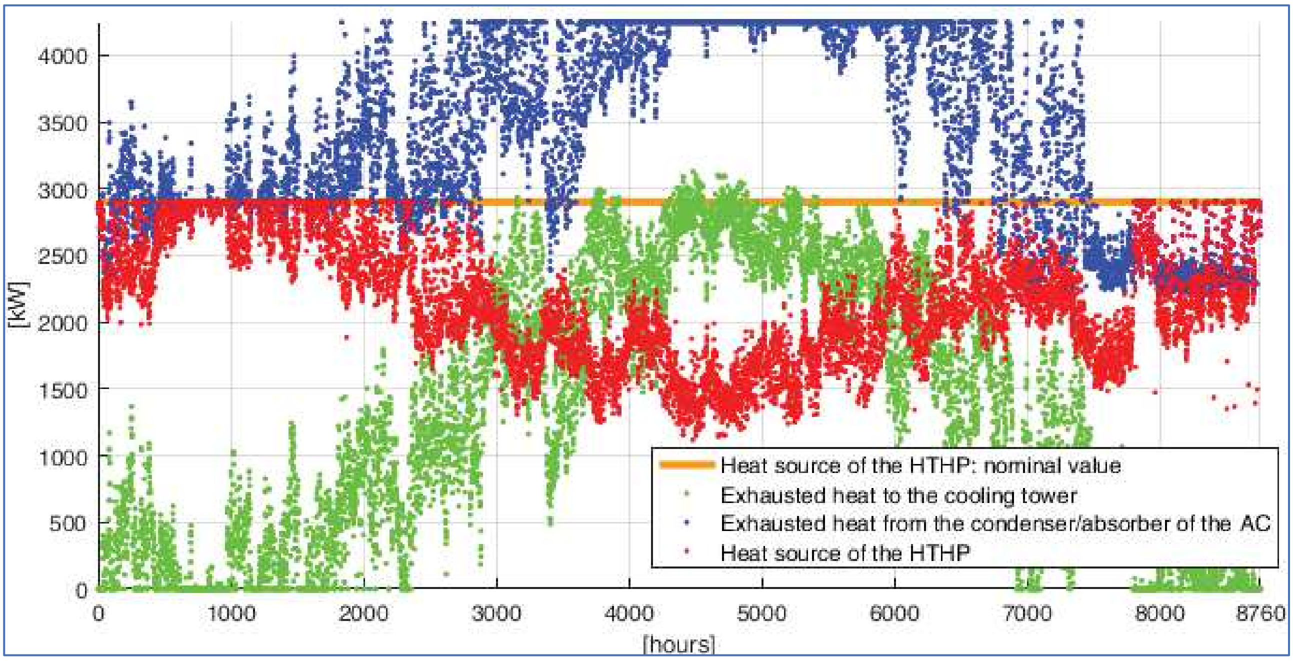

Fig. 18. Optimal operation: interaction between absoprtion chiller, high-temperature heat pump, and cooling tower

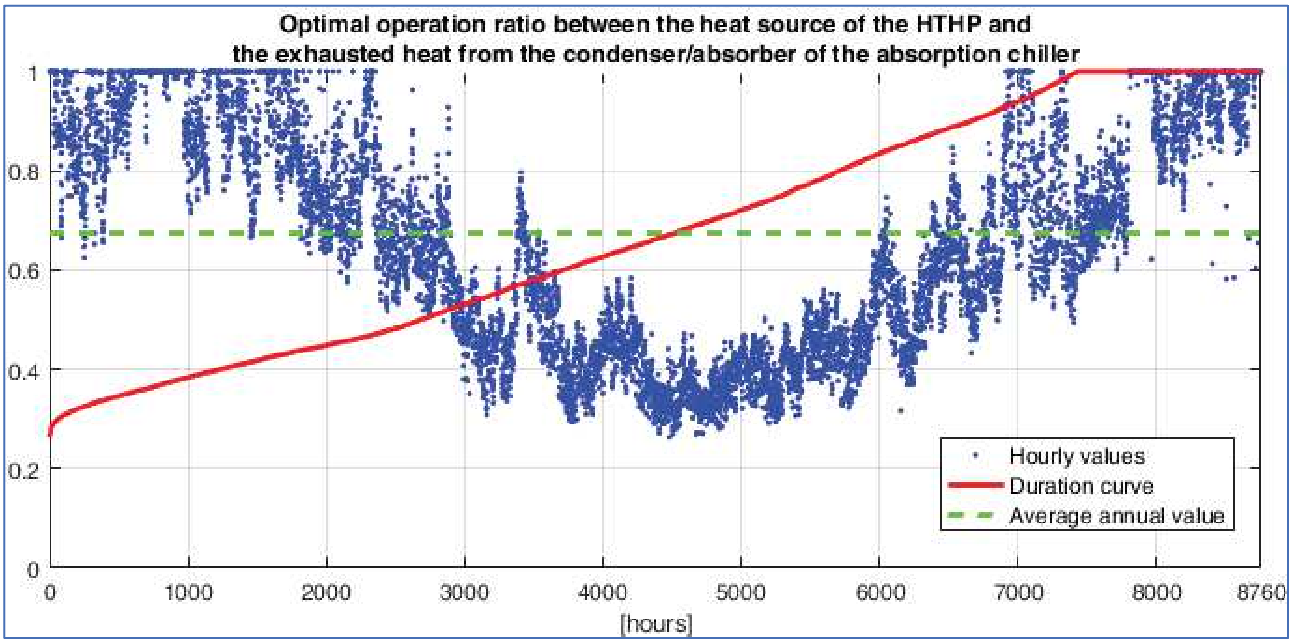

Fig. 19. Optimal operation: ratio between the heat source of the HTHP and the exhausted heat from the condenser/absorber of the absorption chiller

To provide a more in-depth knowledge of the potentialities of the energy system, the stand-alone configuration has been considered as well. No exchange of electricity is allowed (neither selling nor purchasing) with the grid. The Equivalent Annual Cost has been minimized here too and the results are summarized in Table 11.

Table 11

Optimal EAC sizing and operation – stand-alone configuration: results

	CCHP + HP	CCHP	CHP
Internal Combustion Engine	3400 kW	3400 kW	4300 kW
Absorption Chiller	2600 kW	2500 kW	/
High-Temperature Heat Pump	4100 kW	/	/
Boiler: peak heating production	2386 kW	4696 kW	4738 kW
Electric chiller: peak cooling production	3314 kW	4439 kW	5914 kW
Annual Operation Cost	2225 k€	2618 k€	2633 k€
Annualized Investment Cost	492 k€	429 k€	481 k€
Equivalent Annual Cost	**2717 k€**	**3047 k€**	**3113 k€**
Annual Primary Energy Consumption	**55630 MWh**	**65440 MWh**	**65820 MWh**

In this case, the differences between the integrated CCHP-HTHP system and the traditional trigeneration and cogeneration systems become greater, both in terms of economic and energy performances. This means that the integration of a high-temperature heat pump may be suitable and favorable also in stand-alone polygeneration plants, giving enhanced flexibility and resilience to the overall system.

5. Conclusions

The integration of a high-temperature heat pump within a trigeneration system was proposed and analyzed in this paper. The high-temperature heat pump recovers the low-temperature heat from the condenser/absorber of the absorption chiller to produce hot water at around 90 °C, replacing the cooling tower or the air cooler, depending on the case.

A numerical model for the heat pump cycle was developed to assess the performance and operating characteristics of different working fluids and provide the required working conditions. The implementation of an internal heat exchanger was evaluated as well. Ammonia, which achieved a COP of 3.9 at the expected working conditions, was found to be one of the most suitable fluids for this application.

An exergy analysis was also performed to compare the proposed energy system to traditional ones (i.e. separate production, cogeneration, trigeneration). The value of the COP of the high-temperature heat pump was found as a crucial parameter for the exergy performance of the system to be higher than conventional alternatives.

A levelized cost of electricity methodology was adopted to assess the economic viability of the proposed energy system. Results showed that the integration of the high-temperature heat pump within a trigeneration system can be economically profitable compared to conventional technologies.

Finally, a case study was considered. The integration of the proposed trigeneration system into an existing separate-production plant of a pharmaceutical factory was investigated through the economic optimization of the investment. A two-level optimization algorithm was developed: the synthesis/design problem was tackled by means of a genetic algorithm and the operational strategy was optimized by means of a linear programming technique.

The trigeneration system with integrated high-temperature heat pump achieved the best performance, providing the 10.3 %, 10.6 %, and 41.7 % savings in comparison to traditional trigeneration, cogeneration, and separate production systems, respectively. Results also showed that the proposed system provides the flexibility to cover variable energy demands and can achieve favorable performance in terms of annual primary energy consumption and also in stand-alone conditions.

Acknowledgements

The authors acknowledge the Erasmus+ Programme for the financial support to L. Urbanucci for his 3-month research stay at the URV in 2018.

Competing interests

The authors have no competing interests to declare.

Nomenclature

Acronyms

AC	Absorption Chiller
CCHP	Combined Cooling, Heat, and Power
CHP	Combined Heat and Power
GA	Genetic Algorithm
GWP	Global Warming Potential
HTHP	High-Temperature Heat Pump
ICE	Internal Combustion Engine
IHX	Internal Heat Exchanger
LCOE	Levelized Cost of Electricity
LHV	Lower Heating Value
LP	Linear Programming
ODP	Ozone Depletion Potential
SP	Separate Production
VHC	Volumetric Heating Capacity

Parameters

A	Heat transfer area, m^2
CAP	Capacity, MW
COP	Coefficient of performance, dimensionless
CF	Capacity factor, dimensionless
CRF	Capital recovery factor, dimensionless
EAC	Equivalent annual cost, €
f	Cogeneration recovery heat fraction to cooling, dimensionless
R	Natural gas to electricity cost ratio, dimensionless
r	Interest rate, dimensionless
t	Timestep, hour
t_y	Annual operating time, hours
U	Global heat transfer coefficient, $kW/(m^2\,K)$
w	Electric energy consumption per unit of rejected heat, dimensionless
η	Energy efficiency, dimensionless
Ψ	Exergy efficiency, dimensionless

Continuous variables

C	Cooling power, MW
c	Cost per unit of energy, €/MWh
c_{INV}	Investment cost per unit of electric power, €/W
E	Electric power, MW
ech	Chemical exergy per unit of fuel mass, kJ/kg
Ex	Exergy content, MW
ex	Exergy content per unit of mass, kJ/kg
G	Energy content of the consumed fuel per unit time, MW

h	Specific enthalpy, kJ/kg
m	Mass flow rate, kg/s
Q	Heating power, MW
s	Specific entropy, kJ/(kg K)
t	Temperature, °C

Subscripts

0	Dead state environment
AC	Absorption chiller
Av	Avoided
B	Boiler
c	Cooling
C	Cold water
CHP	Combined heat and power
CCHP	Combined cooling, heat, and power
CT	Cooling tower
d	Demand
ICE	Internal combustion engine
E	Electric
EC	Electric chiller
G	Fuel
h	Heating
H	Hot water
HP	High-temperature heat pump
MAINT	Maintenance
Nom	Nominal
p	Purchased from the grid
PE	Purchased electricity
Q	Thermal
Ref	Reference
s	Sold to the grid
SE	Sold electricity
SP	Separate production

References

[1] Aviso KB, Tan RR. Fuzzy P-graph for optimal synthesis of cogeneration and trigeneration systems. Energy 2018;154:258–68.

[2] Afzali SF, Mahalec V. Novel performance curves to determine optimal operation of CCHP systems. Appl Energy 2018;226:1009–36.

[3] Jana K, Ray A, Majoumerd MM, Assadi M, De S. Polygeneration as a future sustainable energy solution - A comprehensive review. Appl Energy 2017;202:88–111.

[4] Sakalis GN, Frangopoulos CA. Intertemporal optimization of synthesis, design and operation of integrated energy systems of ships: General method and application on a system with Diesel main engines. Appl Energy 2018;226:991–1008.

[5] Marquant JF, Evins R, Bollinger LA, Carmeliet J. A holarchic approach for multi-scale distributed energy system optimisation. Appl Energy 2017;208:935–53.

[6] Abdmouleh Z, Gastli A, Ben-Brahim L, Haouari M. Review of optimisation techniques applied for the integration of distributed generation from renewable energy sources. Renew Energy 2017;113:266–80.

[7] Piacentino A, Barbaro C. A comprehensive tool for efficient design and operation of polygeneration-based energy μgrids serving a cluster of buildings. Part II: Analysis of the applicative potential. Appl Energy 2013;111:1222–38.

[8] Ameri M, Besharati Z. Optimal design and operation of district heating and cooling networks with CCHP systems in a residential complex. Energy Build 2016;110:135–48.

[9] Bischi A, Taccari L, Martelli E, Amaldi E, Manzolini G, Silva P, Campanari S, Macchi E. A detailed optimization model for combined cooling , heat and power system operation planning. Energy 2014;74:12–26.

[10] Ma T, Wu J, Hao L, Lee W-J, Yan H, Li D. The Optimal Structure Planning and Energy Management Strategies of Smart Multi Energy Systems. Energy 2018.

[11] Yousefi H, Ghodusinejad MH, Noorollahi Y. GA/AHP-based optimal design of a hybrid CCHP system considering economy, energy and emission. Energy Build 2017;138:309–17.

[12] Soheyli S, Shafiei Mayam MH, Mehrjoo M. Modeling a novel CCHP system including solar and wind renewable energy resources and sizing by a CC-MOPSO algorithm. Appl Energy 2016;184:375–95.

[13] Ghaem Sigarchian S, Malmquist A, Martin V. The choice of operating strategy for a complex polygeneration system: A case study for a residential building in Italy. Energy Convers Manag 2018;163:278–91.

[14] Wang JJ, Jing YY, Zhang CF. Optimization of capacity and operation for CCHP system by genetic algorithm. Appl Energy 2010;87:1325–35.

[15] Li F, Sun B, Zhang C, Zhang L. Operation optimization for combined cooling, heating, and power system with condensation heat recovery. Appl Energy 2018;230:305–16.

[16] Murugan S, Horák B. Tri and polygeneration systems-A review. Renew Sustain Energy Rev 2016;60:1032–51

[17] Jradi M, Riffat S. Tri-generation systems: Energy policies, prime movers, cooling technologies, configurations and operation strategies. Renew Sustain Energy Rev 2014;32:396–415.

[18] Yang G, Zhai X. Optimization and performance analysis of solar hybrid CCHP systems under different operation strategies. Appl Therm Eng 2018;133:327–40.

[19] Maleki A, Rosen MA. Design of a cost-effective on-grid hybrid wind–hydrogen based CHP system using a modified heuristic approach. Int J Hydrogen Energy 2017;42:15973–89.

[20] Kang L, Yang J, Qingsong A, Deng S, Zhao J, Li Z, Wang Y. Complementary configuration and performance comparison of CCHP-ORC system with a ground source heat pump under three energy management modes. Energy Convers Manag 2017;135:244–55.

[21] Leiva-Illanes R, Escobar R, Cardemil JM, Alarcón-Padilla DC. Thermoeconomic assessment of a solar polygeneration plant for electricity, water, cooling and heating in high direct normal irradiation conditions. Energy Convers Manag 2017;151:538–52.

[22] Ommen T, Markussen WB, Elmegaard B. Heat pumps in combined heat and power systems. Energy 2014;76:989–1000.

[23] Al Moussawi H, Fardoun F, Louahlia-Gualous H. Review of tri-generation technologies: Design evaluation, optimization, decision-making, and selection approach. Energy Convers Manag 2016;120:157–96.

[24] Conte B, Bruno JC, Coronas A. Optimal cooling load sharing strategies for different types of absorption chillers in trigeneration plants. Energies 2016;9.

[25] Urbanucci L, Testi D, Bruno JC. An operational optimization method for a complex polygeneration plant based on real-time measurements. Energy Convers Manag 2018;170.

[26] Arpagaus C, Bless F, Uhlmann M, Schiffmann J, Bertsch SS. High temperature heat pumps: Market overview, state of the art, research status, refrigerants, and application potentials. Energy 2018;152.

[27] Bamigbetan O, Eikevik TM, Neksa P, Bantle M, Schlemminger C. Theoretical analysis of suitable fluids for high temperature heat pumps up to 125 °C heat delivery. Int J Refrig 2018;92:185-95.

[28] Ommen T, Jensen JK, Markussen WB, Reinholdt L, Elmegaard B. Technical and economic working domains of industrial heat pumps: Part 1 - Single stage vapour compression heat pumps. Int J Refrig 2015;55:168–82.

[29] Mateu-Royo C, Navarro-Esbrí J, Mota-Babiloni A, Amat-Albuixech M, Molés F. Theoretical evaluation of different high-temperature heat pump configurations for low-grade waste heat recovery. Int J Refrig 2018.

[30] Caf A, Urbancl D, Trop P, Goricanec D. Exploitation of low-temperature energy sources from cogeneration gas engines. Energy 2016;108:86–92.

[31] Tataraki KG, Kavvadias KC, Maroulis ZB. A systematic approach to evaluate the economic viability of Combined Cooling Heating and Power systems over conventional technologies. Energy

2018;148:283–95.

[32] Grassi W. Heat Pumps Fundamentals and Applications. Springer; 2018.

[33] Bell IH, Wronski J, Quoilin S, Lemort V. Pure andPseudo-pure Fluid Thermophysical Property Evaluation and the Open-SourceThermophysical Property Library CoolProp. Ind Eng Chem Res 2014;53:2498–508.

[34] Rees SJ. Advances in Ground-Source Heat Pump Systems. Woodhead Publishing 2016.

[35] LG HVAC Solution Absorption Chiller Catalog. Available at < http://www.lg.com/global/business/download/resources/sac/Catalogue_Absorption%20Chillers_ENG_F.pdf. > [accessed 10.08.2018]

[36] Brunin O, Feidt M, Hivet B. Comparison of the working domains of some compression heat pumps and a compression-absorption heat pump. Int J Refrig 1997;20:308–18.

[37] Choudhari CS, Sapali SN. Performance Investigation of Natural Refrigerant R290 as a Substitute to R22 in Refrigeration Systems. Energy Procedia 2017;109:346–52.

[38] Frate GF, Antonelli M, Desideri U. A novel Pumped Thermal Electricity Storage (PTES) system with thermal integration. Appl Therm Eng 2017;121:1051–8.

[39] Kawasaki Water-Refrigerant Centrifugal Chiller. Available at < https://global.kawasaki.com/en/scope/pdf_e/scope107_03.pdf > [accessed 10.08.2018]

[40] Sabroe HeatPAC (Screw compressor). Available at < http://www.sabroe.com/fileadmin/user_upload/Marketing/Brochures/Heat_pumps/HeatPAC_screw_SB-3571_Jan_2015_GB120dpi.pdf > [accessed 10.08.2018]

[41] Sabroe HeatPAC HPX. Available at < http://www.sabroe.com/fileadmin/user_upload/Marketing/Brochures/Heat_pumps/HeatPAC_HPX_SB-3982_GB120dpi.pdf > [accessed 10.08.2018]

[42] Sabroe HeatPAC (Reciprocating compressor). Available at < http://www.sabroe.com/fileadmin/user_upload/Marketing/Brochures/Heat_pumps/HeatPAC_SB-3982_GB120dpi.pdf > [accessed 10.08.2018]

[43] Neatpump: The High Temperature Ammonia Heat Pump. Available at < http://ammonia21.com/files/448_dvi143_neatpump_en_1209.pdf > [accessed 10.08.2018]

[44] Mayekawa Plus Heat. Available at < http://www.mayekawa.eu/en/media/brochure-downloads/download/13 > [accessed 10.08.2018]

[45] Vijayaraghavan S, Goswami DY. On Evaluating Efficiency of a Combined Power and Cooling Cycle. J Energy Resour Technol 2003;125:221.

[46] Espirito Santo DB do, Gallo WLR. Utilizing primary energy savings and exergy destruction to compare centralized thermal plants and cogeneration/trigeneration systems. Energy 2017;120:785–95.

[47] CEN. Standard EN 15459-1: Energy performance of buildings – Economic evaluation procedure for energy systems in buildings – Part 1: Calculation procedures. European Committee for Standardization 2017. 2017:15459.

[48] Mavromatidis G. Model-based design of distributed urban energy systems under uncertainty. PhD Thesis 2017.

[49] Bejan A, Tsatsaronis G, Moran MJ. Thermal Design and Optimization. John Wiley and Sons Ltd 1995.

[50] Environmental Protection Agency. Catalog of CHP technologies. 2017 Available at < https://www.epa.gov/sites/production/files/2015-07/documents/catalog_of_chp_technologies.pdf > [accessed 10.08.2018].

[51] Environmental Protection Agency. Absorption Chillers for CHP Systems. 2017 Available at < https://www.energy.gov/sites/prod/files/2017/06/f35/CHP-Absorption%20Chiller-compliant.pdf > [accessed 10.08.2018]

[52] Urbanucci L, Testi D. Optimal integrated sizing and operation of a CHP system with Monte Carlo risk analysis for long-term uncertainty in energy demands. Energy Convers Manag 2018;157.

[53] Vogelin P, Koch B, Georges G, Boulouchos K. Heuristic approach for the economic optimisation of combined heat and power (CHP) plants: Operating strategy, heat storage and power. Energy 2017;121:66–77.

[54] CPLEX. Cplex-optimizer. < https://www.ibm.com/analytics/cplex-optimizer > [accessed 10.08.2018]

[55] MATLAB. Genetic Algorithm Solver. < https://it.mathworks.com/discovery/genetic-algorithm.html > [accessed 10.08.2018]